Geophysical Journal International

Geophys. J. Int. (2015) **201,** 406–428
GJI Geodynamics and tectonics

doi: 10.1093/gji/ggv018

Seismic model of the crust and upper mantle in the Scythian Platform: the DOBRE-5 profile across the north western Black Sea and the Crimean Peninsula

V. Starostenko,[1] T. Janik,[2] T. Yegorova,[1] L. Farfuliak,[1] W. Czuba,[2] P. Środa,[2] H. Thybo,[3] I. Artemieva,[3] M. Sosson,[4] Y. Volfman,[1] K. Kolomiyets,[1] D. Lysynchuk,[1] V. Omelchenko,[1] D. Gryn,[1] A. Guterch,[2] K. Komminaho,[5] O. Legostaeva,[1] T. Tiira[5] and A. Tolkunov[6]

[1]*Institute of Geophysics, National Academy of Sciences of Ukraine, Palladin Av.* 32, 03680 *Kiev, Ukraine. E-mail: myronivska@gmail.com*
[2]*Institute of Geophysics, Polish Academy of Sciences, Ks. Janusza* 64, 01-452 *Warsaw, Poland*
[3]*Geology Section, IGN, University of Copenhagen, Øster Volgade* 10, *DK*-1350 *Copenhagen, Denmark*
[4]*Géosciences Azur, Université de Nice Sophia Antipolis, CNRS, IRD, Parc Valrose, F*-06108 *Nice cedex* 2, *France*
[5]*Institute of Seismology, Gustaf Hällströmin katu* 2*B, P.O. Box* 68, *University of Helsinki, FIN*-00014 *Helsinki, Finland*
[6]*State Geophysical Enterprise "Ukrgeofizika", S. Perovskoy str.* 10, 03057 *Kiev, Ukraine*

Accepted 2015 January 12. Received 2015 January 12; in original form 2014 August 11

SUMMARY

The Scythian Platform (ScP) with a heterogeneous basement of Baikalian–Variscan–Cimmerian age is located between the East European Craton (EEC) on the north and the Crimean–Caucasus orogenic belt and the Black Sea (BS) Basin on the south. In order to get new constrains on the basin architecture and crustal structure of the ScP and a better understanding of the tectonic processes and evolution of the southern margin of the EEC during Mesozoic and Cenozoic time, a 630-km-long seismic wide-angle refraction and reflection (WARR) profile DOBRE-5 was acquired in 2011 October. It crosses in a W–E direction the Fore-Dobrudja Trough, the Odessa Shelf of the BS and the Crimean Plain. The field acquisition included eight chemical shot points located every 50 km and recorded by 215 stations placed every ∼2.0 km on the land. In addition, the offshore data from existing profile 26, placed in the Odessa Shelf, were used. The obtained seismic model shows clear lateral segmentation of the crust within the study region on four domains: the Fore-Dobrudja Domain (km 20–160), an offshore domain of the Karkinit Trough at the Odessa Shelf of the BS (km 160–360), an onshore domain of the Central Crimean Uplift (Crimean Plain, km 360–520) and the Indolo-Kuban Trough at the Kerch Peninsula (km 520–620) that is the easternmost part of the Crimea. Two contrasting domains of the ScP within the central part of the DOBRE-5 profile, the Karkinit Trough and the Central Crimean Uplift, may represent different stages of the ScP formation. A deep Karkinit Trough with an underlying high-velocity ($>7.16\,km\,s^{-1}$) lower crust body suggests its rifting-related origin during Early Cretaceous time. The Central Crimean Uplift represents a thick (up to 47 km) crustal domain consisting of three layers with velocities 5.8–6.4, 6.5–6.6 and 6.7–7.0 $km\,s^{-1}$, which could be evidence of this part of the ScP originating on the crust of Precambrian craton (EEC). The thick heterogeneous basement of the Central Crimean Uplift shows inclusions of granitic bodies associated with magmatic activity related with Variscan orogeny within the ScP. General bending and crustal scale buckling of the Central Crimean Uplift with a wavelength of 230 km could be an effect of the Alpine compressional tectonics in the adjacent Crimean Mountains. The extended/rifted continental margin of the ScP (EEC) at the Odessa Shelf and buckling/uplifted domain of the

Central Crimean Uplift affected by compressional tectonics, are separated by the N–S oriented Western Crimean Fault. The crust of the southern margin of the EEC is separated from the ScP, which originated on the EEC crust tectonised and reworked during the Palaeozoic–Mesozoic, by the crustal fault of ∼W–E orientation, which corresponds with the Golitsyn Fault observed at the surface between the EEC and the ScP. The Fore-Dobrudja Domain with a thick (>10 km) heterogeneous basement and two subhorizontal layers in the crystalline crust (with velocities 6.2–6.3 and 6.4–6.65 km s^{-1}) differs from the ScP crust and its origin could be very similar to that of the Trans-European Suture Zone and Palaeozoic West European Platform.

Key words: Controlled source seismology; Wave propagation; Intraplate processes; Continental margins: convergent; Crustal structure; Europe.

1 INTRODUCTION

This paper presents results of the seismic wide-angle refraction and reflection (WARR) experiment along the 630-km-long composite DOBRE-5 profile across the Danube Delta River, the Odessa Shelf and the Crimean Peninsula (Fig. 1). Its objective is to investigate the architecture of the sedimentary cover and the structure of the crystalline crust and uppermost mantle in the region where such information is scarce and old (e.g. fig. 5 in Artemieva & Thybo 2013). The seismic velocity model is based on two data sets (Fig. 1): (1) new onshore WARR data acquired in 2011 October in two areas: in the Dobrudja highlands at the northwestern coast of the Black Sea between the cities of Reni and Kiliya, and (2) on the Crimean Peninsula between the Cape Tarkhankut and the Kerch Peninsula near the Kerch city.

Previously (in the 1960s) acquired offshore (marine) data along the DSS Profile-26, which crosses the Odessa Shelf of the Black Sea from the Zmeinyi Island in the west to the Cape Tarkhankut at the westernmost point of the Crimean Peninsula (Malovitskiy & Neprochnov 1972).

The Scythian Platform (ScP), which has a Baikalian–Variscan–Cimmerian basement age, is located between the southern margin of the East European Craton (EEC) in the north and the Crimean–Caucasus orogenic belt and the Black Sea (BS) Basin in the south (Fig. 2). A commonly accepted tectonic subdivision of the ScP in the study region includes (from west to east) the Fore-Dobrudja Trough, the Odessa Shelf, the Crimean Peninsula Plain with its Central Crimean Uplift, as well as the Azov Sea and the Kerch Peninsula, most of which belongs to the western part of the Indolo-Kuban Trough (Fig. 2; Muratov *et al.* 1968; Ermakov *et al.* 1985; Okay & Tüysüz 1999; Dinu *et al.* 2005; Saintot *et al.* 2006; Khriachtchevskaia *et al.* 2010; Nikishin *et al.* 2011; Seghedi 2012; Munteanu *et al.* 2013).

The sedimentary sequences of this region are well studied by numerous boreholes (published data and data granted by industrial organizations), 2-D and 3-D seismic refraction and reflection studies and seismic tomography investigations carried out since the 1960s.

Systematic geophysical investigations of the Black Sea region by seismic methods began at the end of the 1960s. In the following two decades the BS was covered by a series of deep seismic sounding (DSS) profiles (figs 1 and 5 in Artemieva & Thybo 2013; Neprochnov *et al.* 1970; Malovitskiy & Neprochnov 1972; Moskalenko & Malovitsky 1974; Beloussov & Volvovsky 1989) including the geotraverses III, V, VI and VIII in southern Ukraine (Sollogub *et al.* 1985; Sollogub 1986, 1988a,b; Krasnopevtseva & Schukin 1993) and a deep seismic reflection study (Tugolesov *et al.* 1985; Finetti *et al.* 1998; http://www.blacksea-seismic.com/BlackSeaSPAN). Some of the DSS profiles in the Black Sea have been re-interpreted recently by ray tracing, including the Profile-25 in the western part of the BS and Profile-28/29 in the Azov Sea and the central part of the BS (Yegorova *et al.* 2010), and Profile-26 across the Odessa Shelf (Baranova *et al.* 2011). To better understand the lithosphere structure of the BS, seismological data has recently been re-interpreted to constrain a local seismic tomography model of a part of the Kerch Peninsula with the adjacent part of the BS (Gobarenko *et al.* 2015), and the whole BS area as well (Yegorova & Gobarenko 2010; Gobarenko & Yanovskaya 2011; Yegorova *et al.* 2013).

Recently several seismic experiments under the name of 'DOBRE' have been carried out in southern Ukraine, the Azov Sea and the northern part of the Black Sea. It includes the seismic WARR study and a near vertical reflection study on the NS trending DOBRE'99 profile across the Donbas segment of the Palaeozoic rift basin in southern Ukraine (DOBREfraction 99 Working Group 2003; Maystrenko *et al.* 2003). Later studies addressed the southern extension of the DOBRE'99 line along the NS trending DOBRE-2 line (Fig. 1) across the Azov Sea, the Kerch Peninsula and the Black Sea (Starostenko *et al.* 2015), and the SW–NE trending DOBRE-4 profile between the Fore-Dobrudja Trough and the southern part of Ukrainian Shield (Starostenko *et al.* 2013). To the southwest of the DOBRE-5 profile, seismic data includes the eastern part of the seismic WARR profile VRANCEA 2001 (Hauser *et al.* 2007).

Within the framework of DARIUS programme (istep.dgs.jussieu.fr/darius/) field geological investigations supervised by M. Sosson have been undertaken in the Crimea in order to specify the deformation style and age of the main stratigraphic complexes of the Crimean Mountains (Sheremet *et al.* 2014).

The present results are based on modern technologies for data acquisition and interpretation, providing detailed information on the structure and thickness of the crust in the area which up to now lacked a modern high-resolution crustal-scale seismic model. The new data provide a significant contribution to multidisciplinary research on the lithosphere, in order to understand its structure, origin, and evolution (Artemieva 2011; Percival *et al.* 2012).

2 REGIONAL GEOLOGICAL AND TECTONIC BACKGROUND

The EW trending DOBRE-5 profile traverses the young ScP between the southern margin of the EEC in the north and the Alpine–Mediterranean orogenic belt in the south. The structural and geodynamic development of the region is related to the Vendian–Phanerozoic activation of the southern edge of the craton, and to the evolution of the Palaeo-, Meso- and Neotethys (e.g. Kruglov & Tsypko 1988; Okay *et al.* 1994; Nikishin *et al.* 1998, 2001, 2011;

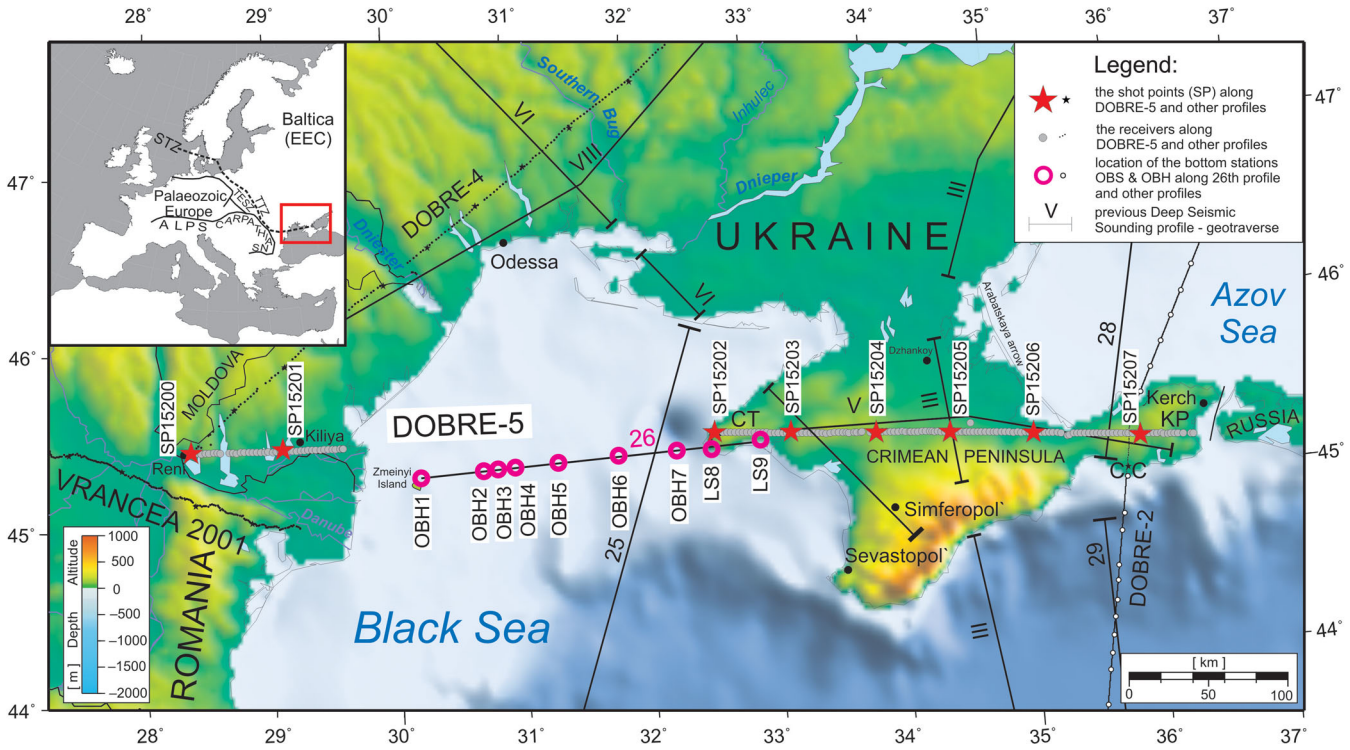

Figure 1. Location of the composite DOBRE-5 profile and previous refraction seismic profiles within the study area. Red stars represent shot points; grey dots—recording stations; red circles—the position of the ocean bottom seismometers (OBS) and ocean bottom hydrophones (OBH) along Profile-26. CC, Cape Chauda; CT, Cape Tarkhankut; KP, Kerch Peninsula; LS8 and LS9, land stations. Inset map shows the location of the study area in Europe. Thin black lines indicate the location of previous seismic lines.

Seghedi 2001, 2012; Saintot *et al.* 2006). The main tectonic units of the study region include the Fore-Dobrudja Trough and the ScP with a heterogeneous folded basement, which includes the Black Sea shelf, the Crimean Peninsula bordered in the southeast by the Crimean Mountains formed as a part of the Crimea–Greater Caucasus orogenic belt, the Azov Sea and the southern slope of the Archean-Lower Proterozoic EEC (Fig. 2). To the south, the deep-water part of the Black Sea is made of two subbasins with a thin high-velocity suboceanic crust or thinned continental crust with a Moho depth of 20–23 km (Starostenko *et al.* 2004; Yegorova *et al.* 2010, 2013).

The Fore-Dobrudja Domain includes the Lower Prut Horst and the Fore-Dobrudja Trough (Fig. 2). The Lower Prut Horst represents a buried fragment of the Alpine/Variscan North Dobrudja orogenic belt separated from the Fore-Dobrudja Trough by the Cahul-Izmail Fault (Slyusar' 1984). The Lower Prut Horst is formed by Palaeozoic–Riphean metamorphosed rocks and early Mesozoic formations, which form a system of NW-trending linear folds, complicated by upthrust–overthrust tectonics (Kruglov & Tsypko 1988; Seghedi 2001, 2012). North Dobrudja, with a basement comprising Palaeozoic metamorphic complexes, records both Variscan and Alpine (Cimmerian) deformation, magmatism and metamorphism (Seghedi 2001, 2012; Balintoni *et al.* 2010) and it is separated from the Central Dobrudja of the Moesia platform by the Pecenega-Camena Fault.

The Fore Dobrudja Trough, located along the border of the EEC and North Dobrudja, has a complex crustal structure as a result of its activation during the Vendian-Mesozoic time (Ermakov & Volfman 1986). In the north, the trough has been formed on a crystalline basement of the EEC and in the south—on the basement of North Dobrudja. It represents an up to 10 km deep inverted Mesozoic basin superimposed on a pre-Triassic, folded Late Neoproterozoic to Devonian strata (e.g. Seghedi 2001, 2012), resting on top of a Neoproterozoic or older crystalline basement. The tectonic origin of the trough is uncertain; it may either be the westernmost segment of the ScP with a basement buried below Cenozoic sedimentary sequences (Seghedi 2001, 2012; Nikishin *et al.* 2003), or a foredeep of North Dobrudja (Khain 1977; Chekunov 1994). Based on borehole data, the sedimentary fill of the basin includes late Neoproterozoic to Permian successions (Seghedi 2001, 2012) and a Mesozoic succession including Triassic clactics and Jurassic black shales and carbonates (e.g. Gazizova 2009; Ivanova 2011). The latter were folded in the Late Jurassic–Early Cretaceous (Hippolyte 2002; Gazizova 2009) and were overlain by an Early–Late Cretaceous through Palaeogene cover (Galetsky 2007; Seghedi 2012).

Further east, the DOBRE-5 profile crosses the ScP on the Odessa Shelf and the Crimean Peninsula. The heterogeneous Baikalian-Cimmerian folded basement (Khain 1977; Kruglov & Tsypko 1988) of the ScP is generally accepted to have been deformed by Variscan tectonics (Muratov *et al.* 1968; Muratov 1969; Milanovsky 1991; Nikishin *et al.* 1998, 2001; Natalín & Şengör 2005). It may have been fully amalgamated to form one major unit by the end-Middle Jurassic (Natal'in & Şengör 2005). At the Romanian Black Sea shelf, the basement is composed of Late Palaeozoic greenshists and younger sedimentary complex of slates, sandstones and limestones, with associated magmatic rocks (Dinu *et al.* 2005). These rock complexes may also represent a slightly tectonized margin of the EEC (Khain 1977; Kruglov & Tsypko 1988; Milanovsky 1996; Okay *et al.* 1996; Robinson *et al.* 1996) which is in agreement with recent studies (Stephenson *et al.* 2004; Gee & Stephenson 2006; Saintot *et al.* 2006) that considered the ScP as a southward

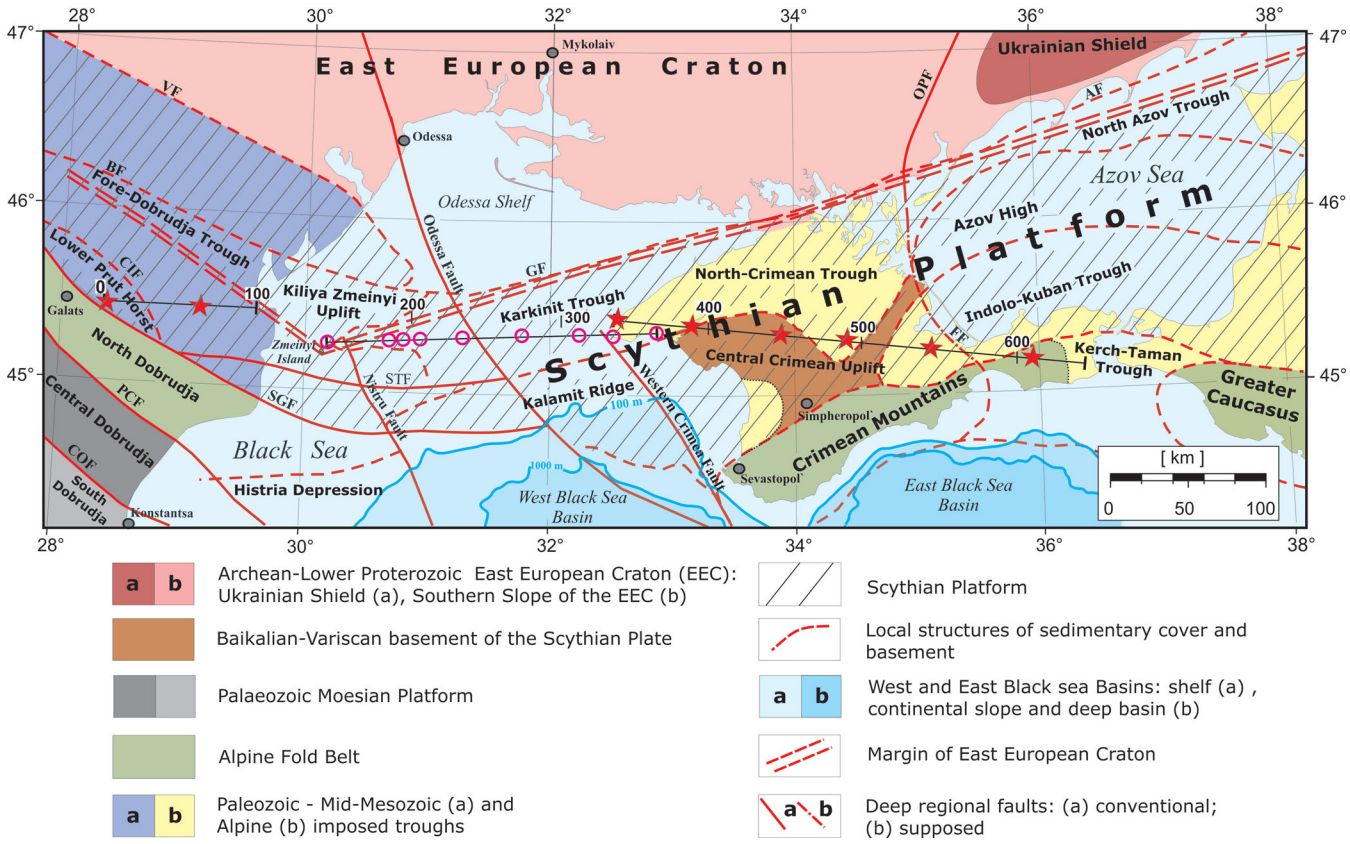

Figure 2. Tectonic map of the Scythian Platform in the region of the DOBRE-5 profile (after Okay & Tüysüz 1999; Dinu *et al.* 2005; Khriachtchevskaia *et al.* 2010; Seghedi 2012; Munteanu *et al.* 2013 with modifications). Deep regional faults: AF, Azov Fault; BF, Bistria Fault; CIF, Cahul-Ismail Fault; COF, Capidava-Ovidiu Fault; FF, Feodosiya Fault; GF, Golitsyn Fault; OPF, Orekhovo - Pavlograd Fault; PCF, Peceneaga-Camena Fault; SGF, Sfantu Gheorghe Fault; STF, Sulina Tarhankut Fault, VF, Vaslui Fault (Sollogub 1986; Dinu *et al.* 2005; Munteanu *et al.* 2011; Seghedi 2012).

continuation of the EEC with the Precambrian basement that has later been reworked by Neo-Proterozoic and Early Palaeozoic tectonic events.

The exact location and nature of the northern, western and southern boundaries of the ScP and of its main units, as well as the precise age of its basement and deep structure, are still poorly known and remain a matter of debate. In the north, the suture zone between an ancient (EEC) and younger (ScP) platform is supposed to follow an east-west trending system of grabens and half-grabens (Kruglov & Tsypko 1988; Saintot *et al.* 2006; Khriachtchevskaia *et al.* 2010; Yegorova *et al.* 2010), probably along a proposed major fault zone, on the Golitsyn and Azov faults (Fig. 2). In the southwest, the ScP is bounded at the south by the Sfantu Gheorghe Fault, separating the Fore-Dobrudja Trough from North Dobrudja (Seghedi 2012), and its eastward continuation offshore (Fig. 2). Further to the east, the southern boundary of the ScP extends somewhere along the continental slope of the deep-water Black Sea basin (Fig. 2).

Within the southern slope of the EEC, the crystalline basement dips gradually southwards from a depth of a few hundred metres to 2–5 km and more (Kruglov & Tsypko 1988). Its offshore southern continuation constitutes the drilled basement of the Odessa Shelf of the Black Sea. Permian red complexes along the southern edge of the continental slope could be indicative of the existence of the Fore-Scythian marginal trough that extends from the Caspian Sea to the south of Fore-Dobrudja, over more than 2000 km in length and about 50–100 km in width (Yudin 2008). However, the presence of Carboniferous—Early Permian strata of Cordilleran Orogen type could also indicate a Permian foredeep molasse complex along the southern margin of the old platform (Nikishin *et al.* 2011).

The Karkinit Trough, a part of the system of rift basins within the ScP, continues eastwards into the North Crimean Trough and the North Azov Trough (Fig. 2), filled with Cretaceous and Palaeogene sedimentary sequences as thick as 3000 m (Khriachtchevskaia *et al.* 2010). In the southern part of the Azov Sea and the major part of the Kerch Peninsula, the Indolo-Kuban Trough has originated, most probably, in the Oligocene–Miocene, contemporaneously with uplift and formation of the Greater Caucasus–Southern Crimean orogen (Denega *et al.* 1998).

The Karkinit and the North-Crimean Troughs, together with the Indolo-Kuban and the Kerch-Taman Troughs, constitute a system of troughs that may define the contact zone between the EEC and the ScP (Fig. 2). They are filled with Oligocene–Quaternary deposits as thick as 6 km (Tugolesov *et al.* 1985). Oligocene-Early Miocene (Maikopian series) molasse dominate in the section of the Indolo-Kuban and Kerch-Taman Troughs. It has been accumulated in the foredeeps of the Crimean Mountains and the North-Western Greater Caucasus due to erosion of material from the slopes of the mountain ridges in the south, and from the Ukrainian Shield in the north (Sidorenko 1969; Nikishin *et al.* 2011). The Karkinit trough is separated from the EEC by the Golitsyn Fault (Fig. 2). In the south the Karkinit Trough terminates at the Kalamit Ridge – basement uplift with Palaeozoic–Jurassic basement covered by thin Cretaceous and Oligocene sedimentary sequences (Denega *et al.* 1998).

The Central Crimean Uplift consists of a chain of local highs separated by small depressions. The basement (Late Baikalian

greenschists of Riphean–Cambrian age (Muratov *et al.* 1968; Kruglov & Tsypko 1988; Nikishin *et al.* 2001) is overlain by rocks of a Variscan complex, which has been low-grade metamorphosed and are comparable to the Karapelit formation of the North Dobrudja and the apex of the Reno-Hercynian region of Western Europe (Muratov *et al.* 1968; Sidorenko 1969). Formations of Carboniferous-Lower Triassic age form the upper part of the Variscan complex classified as upper molasse (Kruglov & Tsypko 1988). Late Palaeozoic magmatism at local highs may be related to Palaeozoic orogenic magmatism in the Caucasus and Dobrudja (Belov 1981). The Cimmerian (Middle Triassic–Middle Jurassic) complex includes terrigenous clay flysch and igneous formations that overlie the basement of the Karkinit and the North Crimean Troughs.

3 SEISMIC EXPERIMENT AND DATA

The total length of the DOBRE-5 seismic profile is 630 km. The coordinates of the westernmost point of the profile (in the region of Reni city) are 45°27′05″N, 28°21′12″E; ending at the Kerch Peninsula (eastern part of the Crimean Peninsula) at the point 45°27′05″N, 28°21′12″E. The field acquisition included new onshore seismic data from chemical shot points on the Crimean Peninsula and Fore-Dobrudja Trough; in addition, the offshore data from existing profile 26, placed in the Odessa Shelf, were used (Fig. 1).

3.1 New on-shore seismic data

The field work involved observation of seismic waves from eight shot points, with two shot points in the Dobrudja region and six shot points on the Crimean Peninsula (Fig. 1). A total of 128 boreholes were drilled to a depth of 25 m each and loaded with a total weight of 6400 kg of TNT (Table 1). The nominal distance between shot points was 50–60 km, and 2.5 km between the receivers. 48 stations were deployed in the Dobrudja region and 150 stations in Crimea. The quality of the data is variable according to local geology conditions and explosion charges. Since the profile DOBRE-5 was acquired with onshore recording of signals from the land shots only, there is a substantial (220 km) gap in the data coverage within the marine part of the profile (Fig. 3). Therefore, to constrain the velocity model in this part, the traveltime curves from analog recordings on Profile-26 (Fig. 1, Malovitskiy & Neprochnov 1972), along DOBRE-5 from the Zmeinyi Island to the Tarkhankut Cape and were digitized and included into the data set (Fig. 4). In addition, the data from two OBHs along this profile were also used.

Seismic *P*-wave phases are correlated along the DOBRE-5 profile for modelling. In general, the traveltime curves coincide within 0.1 s between reciprocal shot points. The observed wavefield (Fig. 3) is represented by seismic phases recorded as first arrivals—refractions from sedimentary layers (P_{sed}), from the upper/middle crystalline crust (P_g) and from the upper mantle (P_n). Later arrivals are represented mainly by reflections from the Moho (P_MP phase). Reflections from the discontinuities in the mid-crustal interval (P_cP) are also observed in some shot records.

3.1.1 *Refractions*

The first arrivals include refractions from the sedimentary sequences, crystalline crust and upper mantle. For most shot points, the first arrivals are traced to offsets of up to 150 km for the P_g phase and about 550 km for mantle phases.

The P_{sed} phases (refractions from the sedimentary strata) are observed with apparent velocities 2.0–2.5 km s^{-1} at offsets of up to 10 km and with a velocity 4.3–4.5 km s^{-1} in the offset range 1–40 km (recorded mostly in the eastern part, e.g., SP 15207). The P_{sed} arrivals often form discontinuous traveltime curves with vertical gaps, which are typical for crustal structures with low-velocity layers. The P_g phase—refractions from the consolidated basement and upper crystalline crust—are observed at 50–120 km offsets with an apparent velocity of 5.5–5.8 km s^{-1}, except for SP 15206, where the apparent velocity reaches 6.2 km s^{-1}. In the eastern part (SP 15207) the P_g phase has an even higher apparent velocity (~7 km s^{-1}).

The mantle phases (mainly P_n arrivals) are observed at offsets >120–150 km with an apparent velocity of 8.2–8.3 km s^{-1}. Strong, high-velocity arrivals with velocities >8.5 km s^{-1}, recorded at SP 15201 at offsets >400 km, are interpreted as reflections from a mantle discontinuity (P_1P).

3.1.2 *Reflections*

The later arrivals represent reflections from crustal discontinuities P_cP (middle crust, top of the lower crust). They are weak and only sporadically observed (e.g. Fig. 3, SP 15204 and 15205). The reflections from the Moho discontinuity (P_MP) are in places difficult to correlate due to a relatively low signal-to-noise ratio. For example, they are invisible for the SP 15204 and diffuse for the SP 15207. This may be due to weak seismic energy generated by these shot points, or by a small velocity contrast at the Moho, which in these regions may possibly represent a transitional/laminated change between crustal and mantle material, rather than a sharp velocity discontinuity. The P_mP reflections are observed at offsets of ~80 km at ~7–9 s reduced traveltime in the western part of the profile (SP 15200) and at offsets >130 km at ~10–11 s reduced traveltime in the eastern part (SP 15207), thus suggesting large variations in crustal thickness along the profile. Strong midcrustal reflections (P_cP) are observed on the section for SP15207, at offsets 30–130 km to W and ~7.5 s reduced traveltime (Fig. 3).

Table 1. Location and parameters of shot points for profile DOBRE-5.

Shot point number	Distance (km)	Latitude N (φ)	Longitude E (λ)	Altitude h (m)	Time UTC (y:d:h:m:s)	TNT charge (kg)
SP15200	1.218	45,451	28,355	60	2011:277:20:12:07.74	1000
SP15201	59.216	45,463	29,097	2	2011:277:20:38:16.79	800
SP15202	331.685	45,448	32,580	79	2011:277:21:10:12.77	600
SP15203	379.853	45,418	33,195	24	2011:277:21:40:47.05	700
SP15204	433.611	45,376	33,879	73	2011:277:22:39:22.30	700
SP15205	480.042	45,343	34,470	63	2011:277:22:12:09.68	800
SP15206	532.203	45,293	35,132	14	2011:278:20:07:39.50	800
SP15207	599.286	45,218	35,981	33	2011:279:20:39:54.90	1000

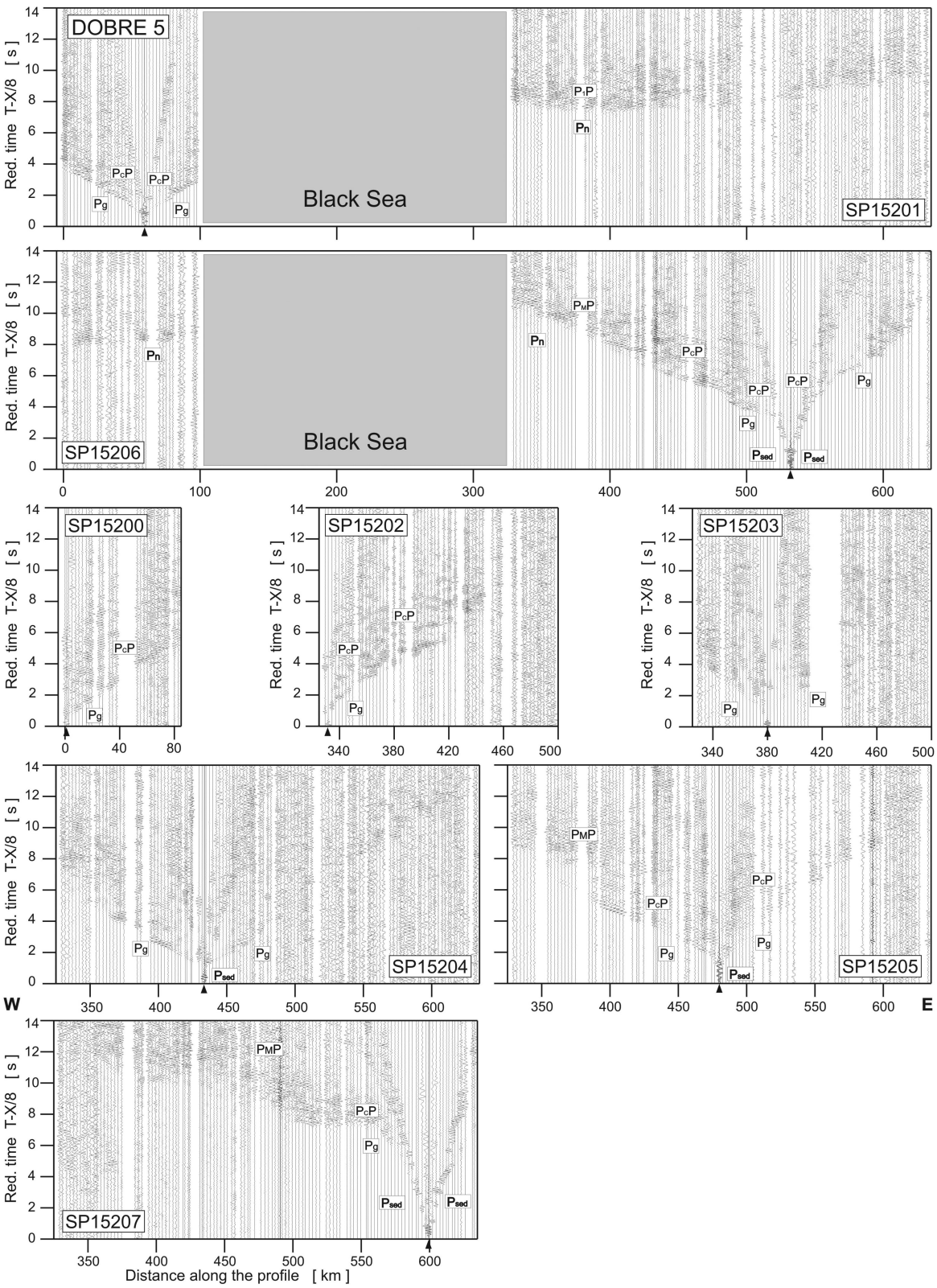

Figure 3. Example of trace-normalized, vertical-component seismic record sections for *P* wave (SP15200 - SP15207) filtered by a bandpass filter (2–12 Hz). P_{sed}, seismic refractions from sedimentary layers; P_g, seismic refractions from the upper and middle crystalline crust; P_{ov}, overcritical crustal phases; P_cP, reflections from middle crustal discontinuities; P_MP, reflected waves from the Moho boundary; P_n, refractions from the sub-Moho upper mantle; P_MP, *P*-wave phases from the upper mantle. The reduction velocity is 8.0 km s^{-1}.

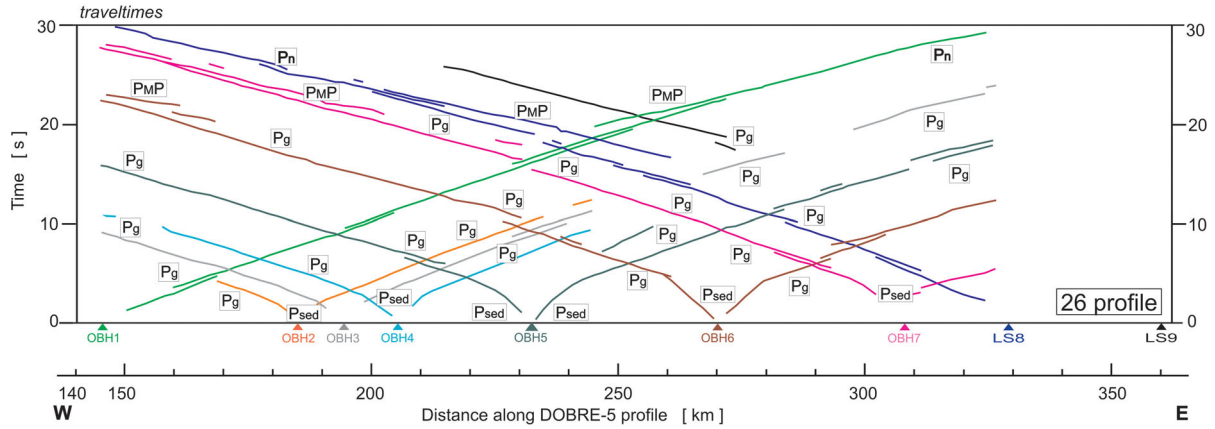

Figure 4. Observed traveltimes recorded along the 26 profile (Malovitskiy & Neprochnov 1972) for OBH1–7 and LS8–9. For abbreviations see Fig. 3.

3.2 Offshore Profile-26

The seismic waves on a 184-km-long DSS Profile-26 recorded in 1966 were generated by chemical shots (explosions) with charges of 105 kg TNT each. These data cannot be reproduced because new ecological regulations prevent new offshore experiments with chemical explosions. The recordings were made by seven ocean bottom hydrophones (OBH 1–7) on the seabed and by two 14-channel analog land stations (LS8 and LS9) placed on the Cape Tarkhankut. The bathymetry along the profile varies from 35 m in the coastal area up to 50 m in its central part (Table 2). Errors in coordinate determination do not exceed a few hundred meters.

In general, the traveltime curves on Profile-26 coincide within 0.1 s between reciprocal points. However, the observation system only allows identification of waves from shallow horizons. There are no P_n phases to determine the depth to the Moho; but a few P_MP phases were identified in the traveltime curves. The digitized traveltimes curves (Fig. 4) cover the offset range of 50–180 km. First arrivals indicate the P_g phase with an apparent velocity of 5.5–6.1 km s^{-1} at 0–100 km offset, possible refractions from the lower crust with a high apparent velocity (~7.1 km s^{-1}) on OBH1, OBH3, and OBH 7–9, and the P_n phase on OBH1 from ~160 km offset. Later arrivals include the P_MP phase (OBH7 and OBH8) and a few short fragments of intracrustal reflections.

4 SEISMIC MODELLING

4.1 Ray tracing modelling strategy

The seismic velocity model along the profile (Fig. 5) was interpreted by trial-and-error forward modelling, using the 2-D ray tracing SEIS83 package (Červený & Pšenčík 1984), the graphical interface MODEL (Komminaho 1998), and ZPLOT (Zelt 1994). The method is based on a high frequency approximation of the wave equation and calculates ray paths, traveltimes and synthetic seismograms. The modeling results are documented in Figs 6–12.

The model consists of layers with the *P*-wave velocity parametrized on an irregular rectangular grid and interpolated by bicubic splines. Layers are separated by velocity discontinuities. During the preparation of the top part of the initial model, geological and geophysical data from boreholes located near the profile and seismic velocities from shallow seismic reflection and refraction profiling (data from Crimean industry organisations) were used to constrain the velocity distribution in the uppermost crust. The top layers were then slightly changed to satisfy the data recorded during this study. Our starting model in the western part of the profile is constrained by the data from four 2.0–5.5 km deep boreholes located within 5.7–28.5 km distance from the profile (Fig. 5). In the eastern part of the profile seventeen 1.5–5.0 km deep boreholes (up to 12.6 km away from the profile) were used. The model was iteratively changed to minimize the traveltime misfit and to obtain similar amplitudes of observed and synthetic data. The model (Fig. 5) was modified until agreement between the observed and calculated traveltimes and amplitudes for the main phases were achieved (Figs 6–10). The seismic modelling was done using seismic record sections with different parameters like filters and velocity reductions or zooms on large computer displays. The seismic sections presented at the scale available in the publication do not show all details of the modeled wavefield.

Table 2. Location of receiving points along DSS profile 26.

Point ID	Distance (km)	Latitude N (φ)	Longitude E (λ)
OBH1	145.334	45,26922	30,20504
OBH2	184.860	45,29478	30,70751
OBH3	194.190	45,30050	30,82618
OBH4	205.057	45,30700	30,96443
OBH5	232.414	45,32262	31,31261
OBH6	270.298	45,34250	31,79506
OBH7	308.243	45,36038	32,27862
LS8	329.345	45,34505	32,54900
LS9	360.350	45,38158	32,94310

Note: OBH, ocean bottom hydrophone; LS, land station.

4.2 Resolution analysis of the ray tracing model

GPS techniques were used to record the shot times and locations of the shots and receivers, with an accuracy of *ca.* 1 ms and tens of metres, respectively. Such errors are insignificant in a crustal-scale experiment. Uncertainties of velocities and depths in the model obtained by the ray tracing technique result, first of all, from the uncertainties of the picked traveltimes which are of the order of 0.1 s. However, the accuracy changes with quality and amount of data, that is number of shots and receivers, effectiveness of sources, signal-to-noise ratio, reciprocity of traveltime branches and ray coverage in the model.

The resolution of the model has been tested by checking the fit between theoretical and observed (experimental) traveltimes for

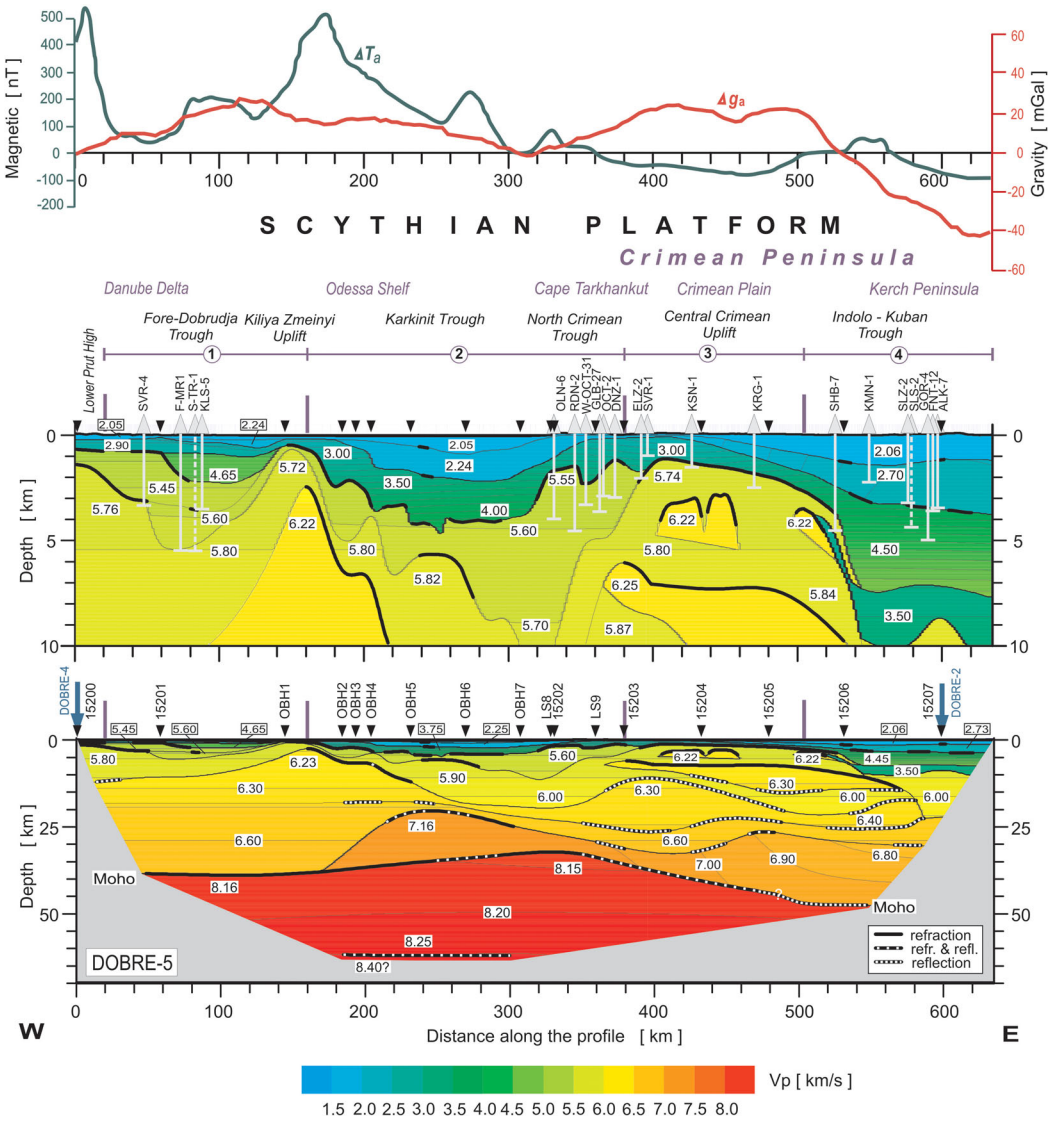

Figure 5. 2-D model of seismic *P*-wave velocity along the DOBRE-5 profile in the sedimentary cover (middle diagram) and the crust and upper mantle derived by forward ray tracing modelling (bottom diagram) using the SEIS83 package (Červený & Pšenčík 1984). Black lines represent velocity discontinuities and thick black lines mark zones where reflected or/and refracted arrivals constrain the discontinuities. Thin lines represent velocity contours with values in km s^{-1} shown in white boxes. The position of tectonic units is indicated. Defined crustal blocks are indicated by numbers in circles: 1 – Fore-Dobrudja Domain, 2 – Karkinit Trough, 3 – Central Crimean Uplift, 4 – Indolo-Kuban Trough. Black arrows show the positions of shot points. Blue arrows show intersections with other profiles. Vertical exaggeration is ~14.5:1 for the sedimentary cover model, and ~2.4:1 for the whole model. Boreholes (data from industry organisations): SVR-4, Suvorovskaya (13.2 km to north from the profile); FMR1, Furmanovskaya (5.7 km to N); S-TR-1, Staro-Troyanovskaya (28.5 km to N); KLS-5, Kiliyskaya (16.0 km to N); OLN-6, Olenevskaya (2.8 km to S); RDN-2, Rodnikovskaya (0.8 km to S); W-OCT-31, Zap.-Oktyabrskaya (1.6 km to S); GLB-27, Glebovskaya (9.6 km to N); OCT-2, Oktyabrskaya (2.8 km to S); DNZ-1, Donuzlavskaya (5.0 km to N); ELZ-2, Elizavetinskaya (0.6 km to S); SVR-1, Severskaya (7.2 km to N); KSN-3, Krasnovskaya (5.8 km to N); KRG-1, Krasnogvardeiskaya (12.6 km to N); SHB-7, Shubinskaya (1.6 km to N); KMN-1, Kamenskaya (1.4 km to N); SLZ-2, Seleznevskaya (2.0 km to N); SLS-2, Sliusarevskaya (1.6 km to S); GOR-4, Gornostaevskaya (3.1 km to N); FNT-12, Fontanovskaya (0.4 km to N); ALK-7, Alekseevskay (0.4 km to N). Bouguer gravity and total magnetic field anomalies along the DOBRE-5 profile are shown on top diagrams (Khomenko 1987; Kruglov 2001).

both refracted and reflected waves. Several modeling tests were performed following similar studies (Janik *et al.* 2002; Grad *et al.* 2003, 2006a; Środa *et al.* 2006). In one test we calculated that the traveltimes for the *P*-wave velocity in one crustal layer varied by ±0.1 km s^{-1} and the Moho depth varied by ±2 km. It is evident (Fig. 11), that the accuracy of our model is better than these values. Diagrams showing theoretical and observed traveltimes for all phases along the profile, ray coverage and traveltime residuals from forward modelling (Fig. 12) show a good agreement between observed and calculated data, with some unimportant exceptions. The rms misfit values for the onshore part of the profile (0.31 s for the crust, 0.15 s for the P_MP, P_n and the upper mantle phases) are considered to be acceptable.

The rms misfit is 0.20 s for the refracted branches in the crust, and –0.37 s for reflected branches. The overall rms misfit is 0.29 s for 1095 picks. It means that velocities in the crust, determined mainly from refracted waves, are better modelled than depths of boundaries determined mainly from reflections.

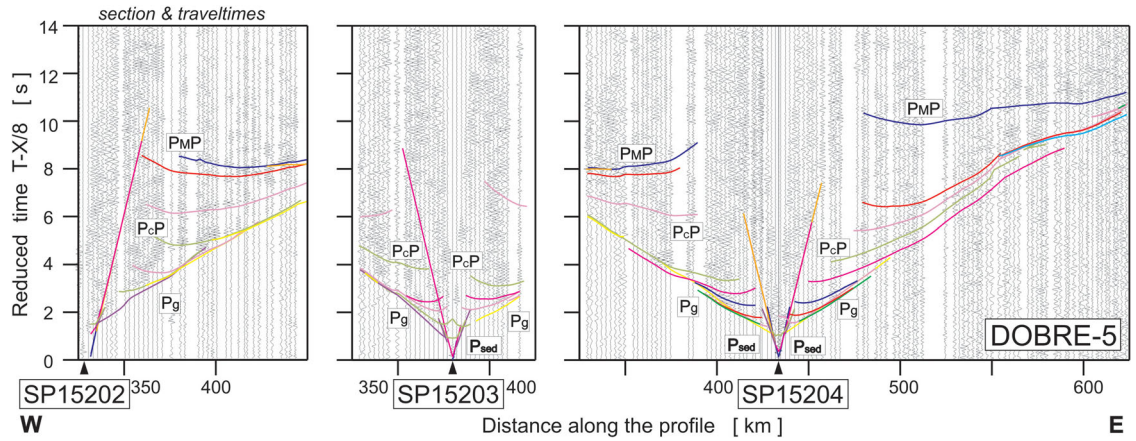

Figure 6. Example of seismic modelling results for SP15202, SP15203 and SP15204. The seismic record sections (amplitude-normalized vertical component) are superimposed by theoretical traveltimes calculated using the SEIS83 ray tracing technique for the model (Fig. 5). Data has been filtered with the 2–12 Hz bandpass filter and displayed with the reduction velocity of 8.0 km s^{-1}. For abbreviations see Fig. 3.

The uncertainty of the Moho depth is less than for intracrustal boundaries.

The structure of the uppermost mantle is also well determined. Picks and some data digitized from Profile-26 located slightly off the DOBRE-5 profile were tested against our model and slightly modified based on the new data. The rms misfit values are 0.15 s for first arrivals and 0.18 s for the P_MP phase (limited to stations 7 and 8 where picks for that phase were available). Thus it is clear that the offshore segment of the model is well determined despite the questionable quality of the digitized old offshore data.

5 *P*-WAVE VELOCITY MODEL OF THE CRUST

5.1. Sedimentary cover and crustal layers

The sedimentary cover consists of layers with a strongly varying thickness and *P*-wave velocity ranging from 1.9 to 4.65 km s^{-1}. The depth to the basement ranges from 1 to 5 km in the basement highs (the Kiliya-Zmeinyi Uplift and the Central Crimean Uplift) which separate three major areas of sediment accumulation, to 10–12 km within the Karkinit and Indolo-Kuban Troughs (Figs 5 and 13). The top of the crystalline basement is marked by a seismic interface to a layer with V_p = 6.2–6.4 km s^{-1}, which we associate with the top of pre-Riphean complexes. It deepens from 3 to 5 km below the Kiliya-Zmeinyi Uplift to 20–22 km in the Indolo-Kuban Trough, although it may be much shallower beneath the Central Crimean Uplift. *P*-wave heterogeneity indicates that the inner structure of the ScP basement is complex, which may be caused by the presence of the Baikalian, Variscan and Cimmerian complexes of different degrees of metamorphism.

The resulting velocity model of the DOBRE-5 profile (Figs 5 and 13) includes three layers in the crystalline crust: the upper crust (V_p = 6.20–6.40 km s^{-1}), the middle (V_p = 6.50–6.70 km s^{-1}) and the lower (V_p = 6.80–7.20 km s^{-1}) crust. In addition, two uppermost crustal layers with velocities 5.55–5.9 and 6.2–6.38 km s^{-1} and with strongly undulating interfaces were detected. The uplifts of these layers of up to 1–4 km depth make the Kiliya-Zmeinyi basement uplift at the Odessa Shelf and the Central Crimean Uplift within the Crimean Plain. In comparison with the western part of the profile, the eastern part has a complex upper crustal structure with a number of high-velocity bodies beneath the Central Crimean Uplift. The mid-lower crust is 10–20 km thick and includes high-velocity lower crustal bodies ($V_p \sim$ 7.15 km s^{-1}) with a maximum thickness of 15 km at distances from km 160 to 440 along the profile (the Karkinit Trough). The velocity at the top of the HVLC is documented quite well by refracted waves recorded on sections for OBH1 (see Fig. 7), OBH3, and OBH7–9. The situation that reversed traveltimes with an apparent velocity higher than 7 km s^{-1} show in first arrivals on observed traveltimes is rare. From the modelling, we know that the velocities in the lower crust to the west and to the east from the HVLC are lower, but accuracy of its determination, because of absence of enough data, is low. We can expect values of V_p at the band of 6.8 and 7.0 km s^{-1}. In our model, velocities are extrapolated from crossing profiles, DOBRE-4 (Starostenko *et al.* 2013) in the western part and DOBRE-2 (Starostenko *et al.* 2015) in the eastern part of the profile. However, at the distance 480 km, $V_p \sim$ 6.9 km s^{-1} is confirmed by refraction on the SP15207 section.

5.2. Moho boundary and upper mantle

The velocity model (Fig. 5) indicates strong lateral variation in crustal structure and Moho topography. This result is in agreement with previous studies which indicated considerable Moho undulations in the region (Sollogub *et al.* 1985; Sollogub 1986). To the west from km 160, the Moho is relatively flat at a depth of ≈38 km. Eastwards, the Moho shallows to 33 km at km 340, and dips significantly to a depth of 47 km (at km 520) in the eastern part of the profile. The sub-Moho velocities are homogeneous, *ca.* 8.15 km s^{-1}. A subhorizontal reflector in the upper mantle beneath the Karkinit Trough was detected about 25 km below the Moho at a depth of ∼60 km, *cf.* the record sections of SP15201 and SP15206 (Figs 9 and 10). The uppermost mantle *P*-wave velocities gradually increase with depth from 8.15 to 8.25 km s^{-1} at a seismic boundary 65 km deep.

6 GEOLOGICAL AND TECTONIC INTERPRETATION

The ScP basement is covered by sedimentary strata of different age, lithology and deformation style. The same lithological and stratigraphic units may have a different velocity depending on depth and location, and similarly, layers with similar velocities often correspond to sedimentary sequences of a different age. Similar observations have been made in the velocity model of the DOBRE-

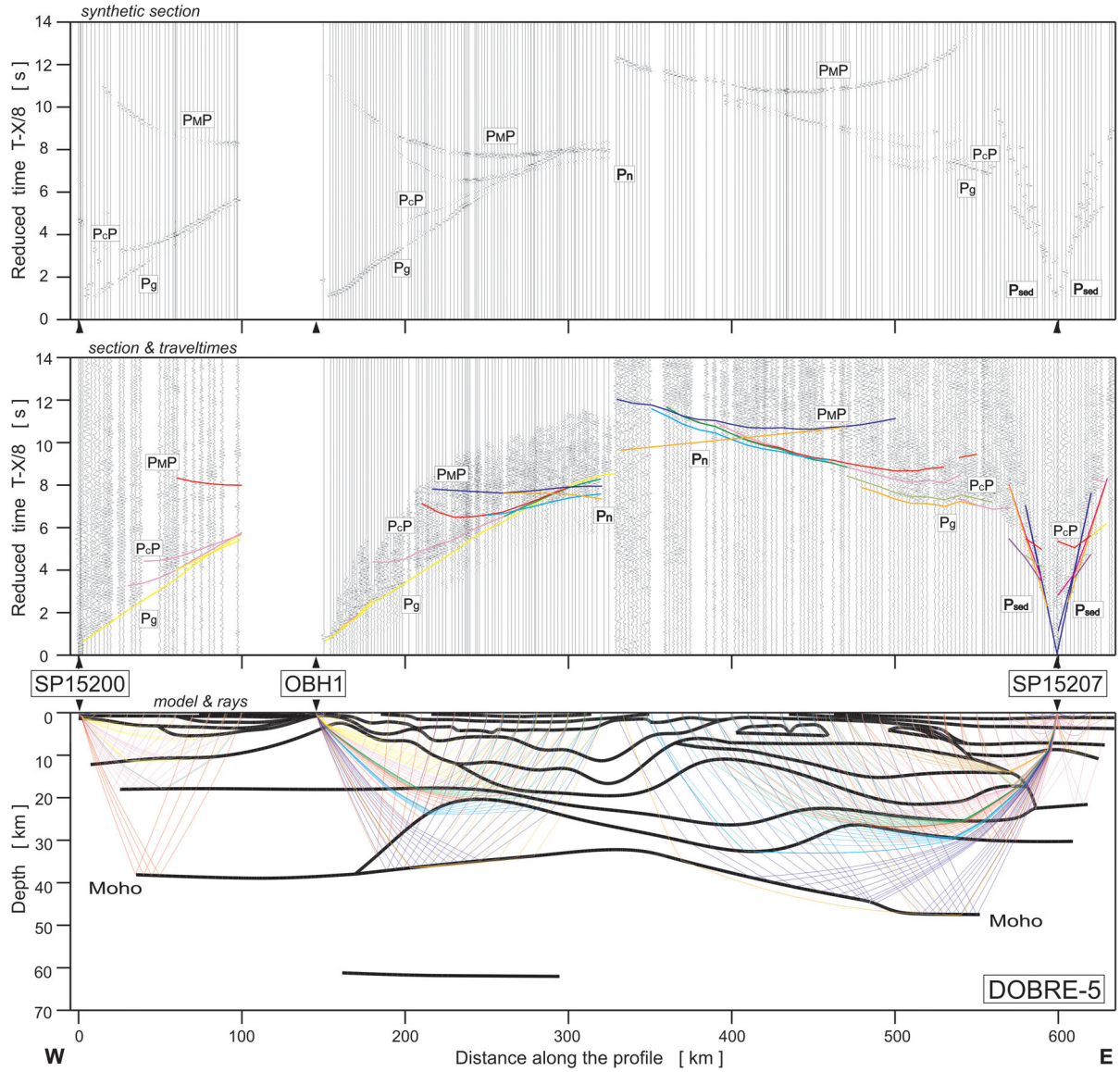

Figure 7. Example of seismic modelling results for SP15200, OBH1 and SP15207: Synthetic seismograms (top diagram); Seismic record sections (amplitude-normalized vertical component) with theoretical traveltimes calculated using the SEIS83 ray tracing technique (data has been filtered with the 2–12 Hz bandpass filter and displayed with the reduction velocity of 8.0 km s^{-1}; central diagram); and ray diagram of selected rays using the SEIS83 (bottom diagram). All examples were calculated for the model presented in Fig. 5. The record section for OBH1 presents digitized pieces from the old paper sections. The beginning of digitization starts *ca.* 2 s before 'real' first arrivals and represents noise level. For abbreviations see Fig. 3.

4 profile (Fig. 1) at the transition between the EEC and Northern Dobrudja (Starostenko *et al.* 2013). The heterogeneous basement of the ScP along the DOBRE-5 line is interpreted as the layer with $V_p > 5.72$–5.82 km s^{-1}.

6.1 Major crustal blocks

The profile DOBRE-5 crosses the main tectonic units of the ScP, which represent complex mosaics of basement segments of Baikalian and Phanerozoic ages outside the southern margin of the EEC. The *P*-wave velocity model along the DOBRE-5 profile (Fig. 5) shows from west to east a clear segmentation of the crust into four blocks, which are discussed in detail in Sections 6.2–6.5:

(i) The Fore-Dobrudja Domain (km 20–160).

(ii) The Odessa Shelf of the Black Sea including the Karkinit Trough (km 160–380).

(iii) The Central Crimean Uplift (km 380–505).

(iv) The Indolo-Kuban Trough at the Kerch Peninsula (km 505–620).

The domains are separated by major faults (Fig. 2 and Section 6.6). The segmentation of seismic crustal domains along the DOBRE-5 profile correlates with the patterns of the gravity and magnetic fields (Fig. 5, upper panel; Khomenko 1987; Kruglov 2001).

At the western end of the profile, weakly positive magnetic anomalies of the Fore-Dobrudja Trough terminate at the Lower Prut Horst and the Northern Dobrudja, which have a strong magnetic anomaly (Fig. 5). A similar strong positive magnetic anomaly is associated with the basement high of the Kiliya Zmeinyi

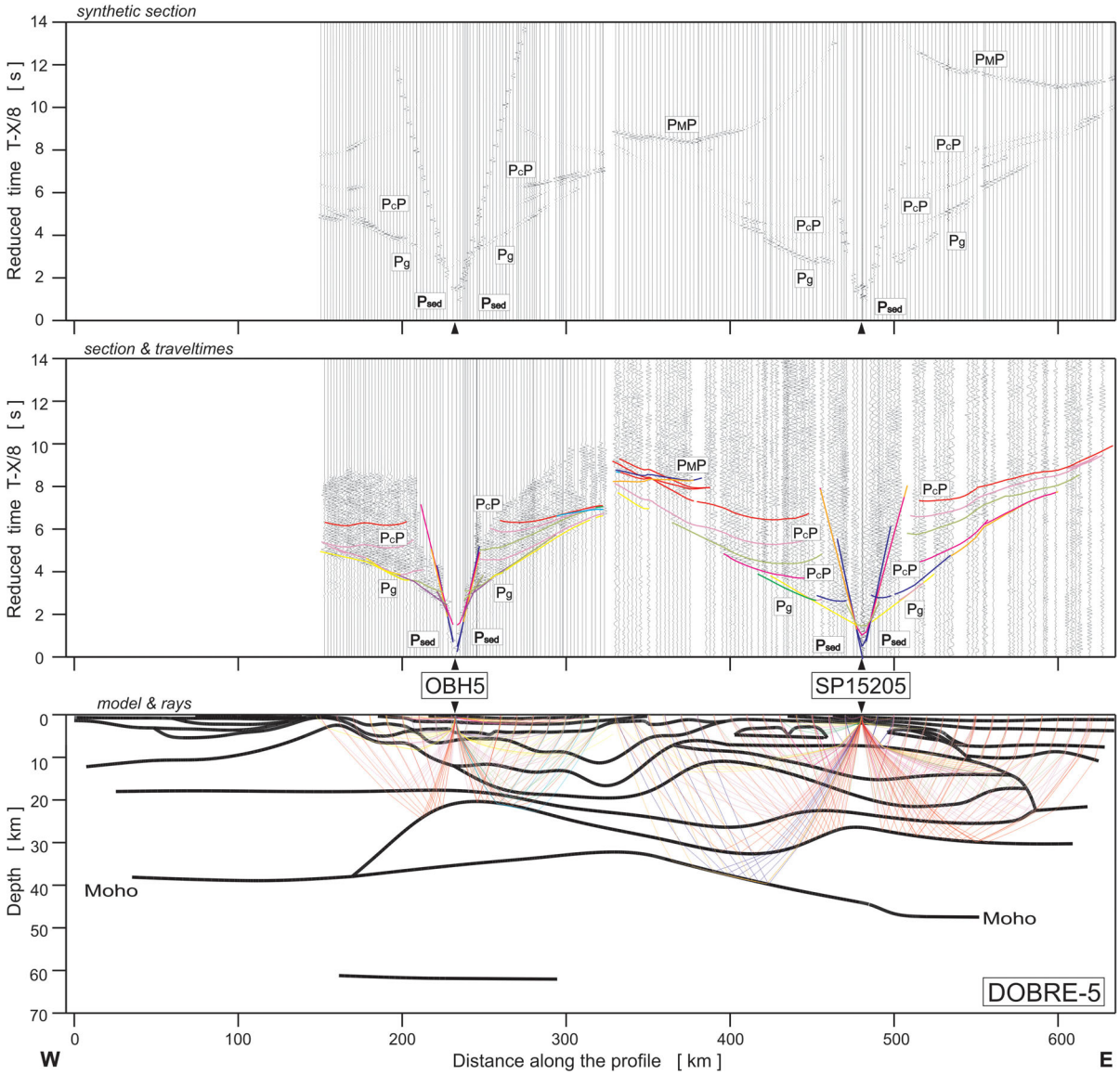

Figure 8. Example of seismic modelling results for OBH5 and SP15205. See caption to Fig. 7 for explanation.

Uplift. Much smaller positive magnetic anomalies are observed within the Fore-Dobrudja and the Karkinit Trough. The latter is a part of the linear north–south trending Odessa magnetic anomaly, which may be caused by magnetic sources in the Precambrian basement of the southernmost EEC (Yegorova & Gobarenko 2010; Starostenko *et al.* 2014). The magnetic field of the Central Crimean Uplift and the Kerch Peninsula is negative (*ca.* –80 nT magnitude), suggesting either that the magnetic layer is very deep, in agreement with our interpretation of a thick Cimmerian sequence there, or that lithospheric temperatures are high, as the presence of a recent mud volcanism activity in the Kerch Peninsula region suggests.

The Bouguer anomaly is slightly positive below of the Karkinit Trough. It is remarkable that the shallowest Moho corresponds to a gravity low (Fig. 5) between the Odessa Shelf and Crimea. The major part of the Central Crimean Uplift is characterized by a weakly positive (+20 mGal) gravity anomaly, located at the northern peripheral zone of a +100 mGal gravity anomaly in the Crimean Mountains (fig. 4 in Yegorova & Gobarenko 2010). Low gravity field (−40 to −50 mGal) in the Kerch Peninsula and the Indolo-Kuban Trough may probably be caused by the thick Cenozoic sedimentary sequences (Fig. 5).

6.2 The Fore-Dobrudja Domain (km 20–160)

6.2.1 Sedimentary cover

The Fore-Dobrudja Trough has been drilled by a number of boreholes down to the depth of *ca.* 5.5 km. (Patrut *et al.* 1983; Slyusar' 1984; Papanikolaou *et al.* 2004; data from Crimean industry organisations). The sedimentary cover, ranging in thickness from 4 to 12 km, is characterized by complicated lithology and stratigraphy (Figs 5 and 13; Slyusar' 1984; Dinu *et al.* 2002, 2005; Seghedi 2012). The uppermost part consists of Miocene–Quaternary ($V_p = 2.05\,\mathrm{km\,s^{-1}}$) and Eocene–Oligocene ($V_p = 2.24\,\mathrm{km\,s^{-1}}$) sedimentary sequences above Eocene marls, which are underlain by Jurassic–Cretaceous strata ($V_p = 2.90\,\mathrm{km\,s^{-1}}$) of 500–700 m thickness. The gradual change in sedimentation environment from the Middle Jurassic deep-water formations to lagoonal and continental

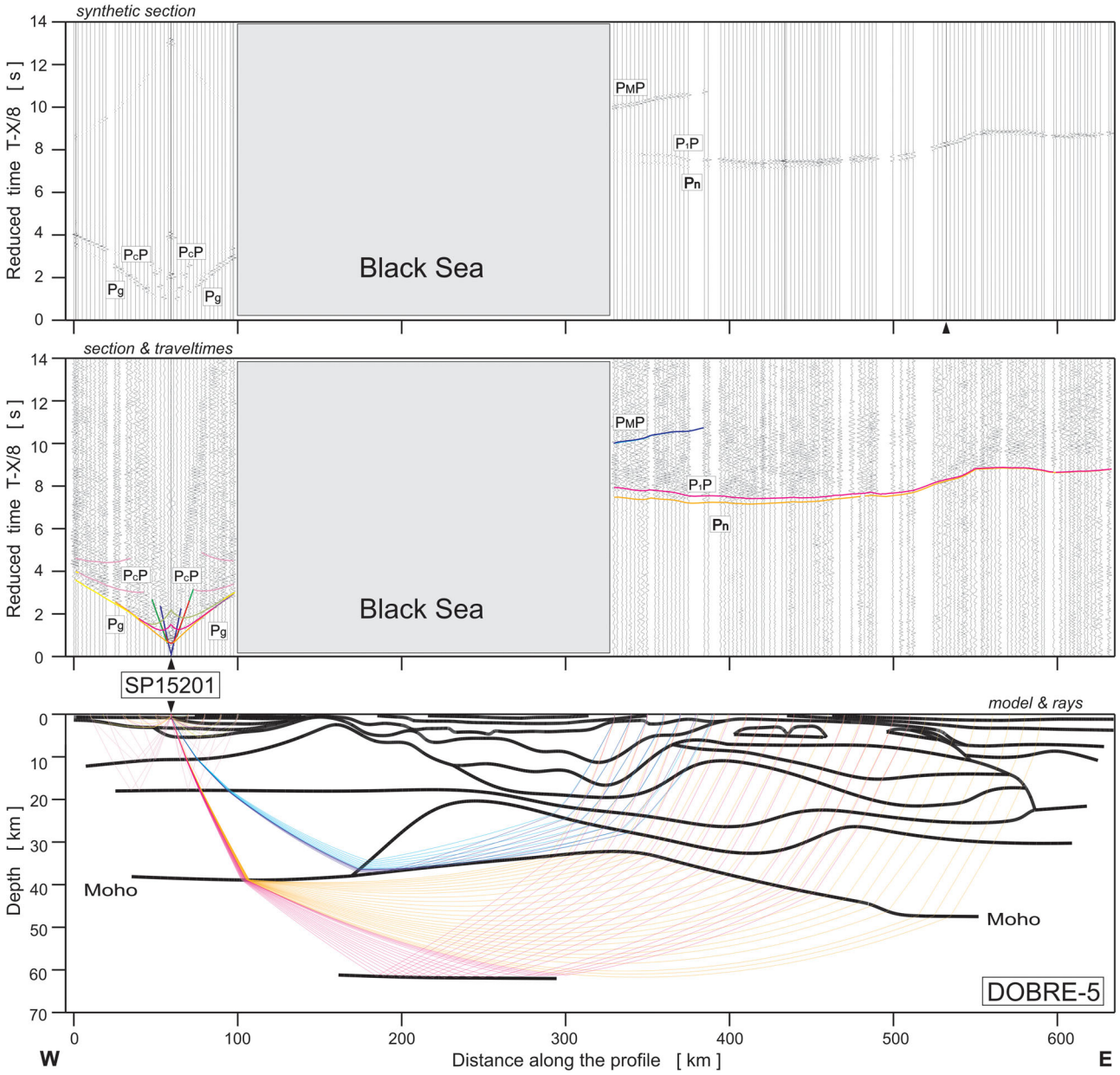

Figure 9. Example of seismic modelling results for SP15201. See caption to Fig. 7 for explanation.

clastic-carbonate and sulpfate-halogen deposits of Lower Cretaceous age suggests gradual uplift of this area during the final stage of Cimmerian collisional tectonics.

The Variscan formations of the Fore-Dobrudja Trough include the Triassic terrigenous clay complex ($V_p = 4.65\,\mathrm{km\,s^{-1}}$), Permian red volcano-clastic rocks ($V_p = 5.45\,\mathrm{km\,s^{-1}}$) and the Middle Devonian-Carboniferous sulpfate-carbonate complex ($V_p = 5.60\,\mathrm{km\,s^{-1}}$), which all together amount to *ca.* 4 km in thickness. The Middle Carboniferous-Lower Triassic part of the section may be related to the Karapelit formation of the Mechin zone (red and grey coal-bearing molasses, effusive rocks and volcano-clastics of a different composition; Kruglov & Tsypko 1988). The platform complexes of Upper Palaeozoic sediment sequences of the Fore-Dobrudja Trough may correspond to coeval strata in the North Dobrudja, which were deformed during the Baikalian-Variscan collisional tectonics (Ermakov *et al.* 1985; Kruglov & Tsypko 1988). However, the boundary between the North Dobrudja and the Fore-Dobrudja Trough is not revealed in the velocity models on both the profiles DOBRE-5 (Fig. 5) and DOBRE-4 (Starostenko *et al.* 2013).

The lowermost part of the sedimentary strata, an 8–10-km-thick layer at a depth interval from *ca.* 4–5 km down to 10–12 km, is not penetrated by boreholes and its structure is known only from remote geophysical surveys. It is supposed (Slyusar' 1984) to consist of carbonates and terrigenous formations of the Vendian–Lower Devonian complex, which overlie migmatites, plagiogranites and shales of the Riphean basement. The oldest sediments found in this area consist of Vendian–Lower Cambrian sandstones, tuffs and argillaceous tuffs (Patrut *et al.* 1983; Dinu *et al.* 2005). The velocity model shows no difference between the Devonian rocks and the Riphean basement (Fig. 5) with $V_p = 5.72$–$5.80\,\mathrm{km\,s^{-1}}$. The basement of the Lower Prut Horst, a northwest dipping part of the North Dobrudja (km 0–70 km), is composed of Late Proterozoic crystalline schists and greenschists of Riphean–Lower Cambrian age, terrigenous carbonate formations of Silurian–Lower Devonian and

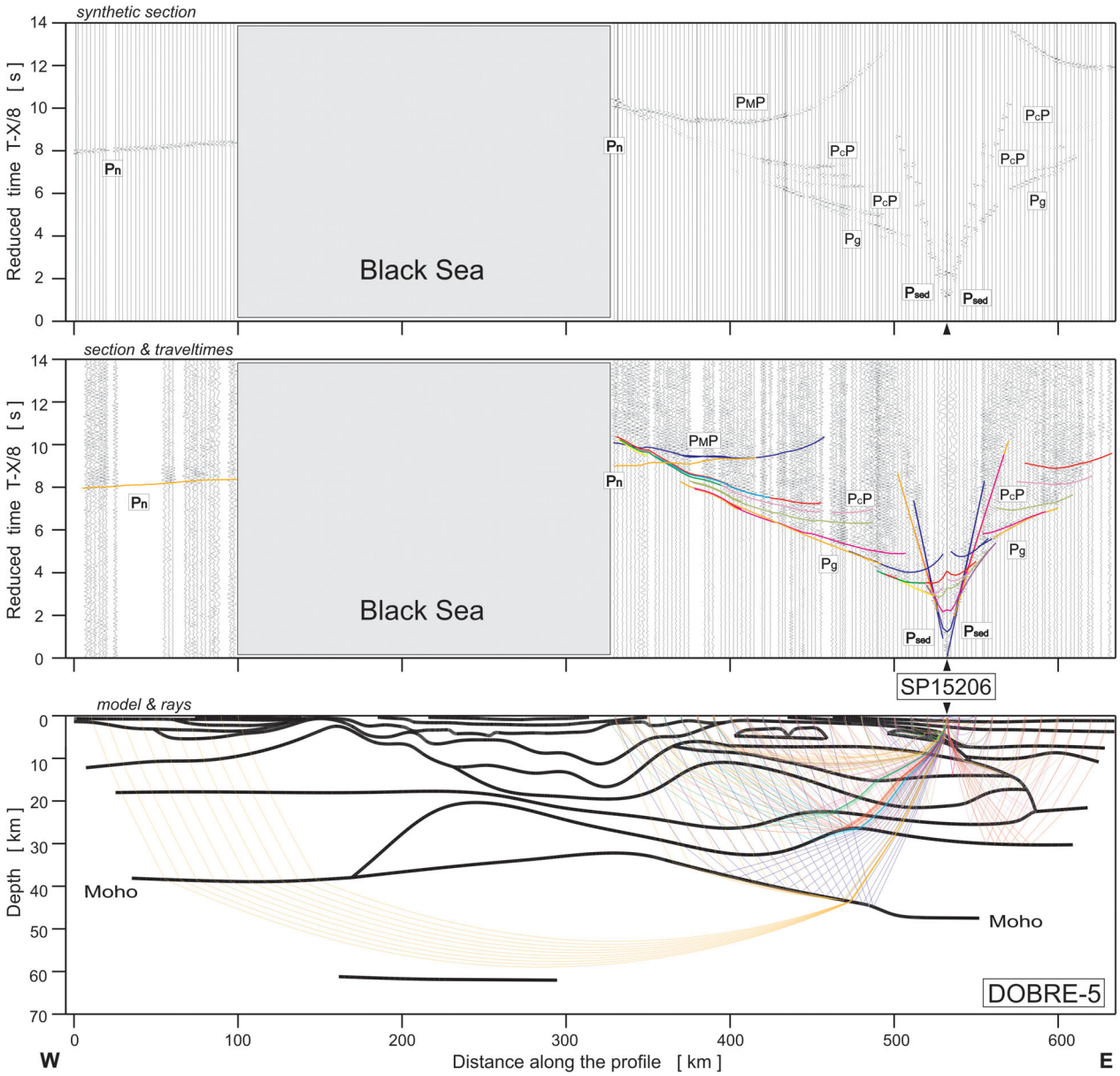

Figure 10. Example of seismic modelling results for SP15206. See caption to Fig. 7 for explanation.

Middle–Upper Devonian carbonate deposits ($V_p = 5.76$–5.8 km s^{-1}; Slyusar' 1984; Dinu *et al.* 2002, 2005; Seghedi 2012).

The Carboniferous-Lower Triassic red deposits are associated with the top of the basement (Kruglov & Tsypko 1988; Nikishin *et al.* 2011). Baikalian–Variscan formations of the North Dobrudja are strongly metamorphosed and deformed in narrow northwest and west–east trending linear folds, which are complicated by upthrusts and overthrusts of northeastern vergence (Ermakov *et al.* 1985; Kruglov & Tsypko 1988). The heterogeneous basement of the Fore-Dobrudja Trough also includes the Riphean complexes (migmatites, plagiogranites and schists) and the Vendian-Lower Devonian formations of the Transnistrian pericratonic trough, which is the southwesterly dipping edge of the EEC.

6.2.2 *Crystalline crust*

In contrast to the ScP (discussed below), the Fore-Dobrudja Trough has a two-layered crystalline crust, which is very typical for a velocity structure of Palaeozoic West European Platform (Meissner 1986; Aichroth *et al.* 1992; Jensen *et al.* 2002; Artemieva & Meissner 2012), although the crust is thicker with the Moho at 38–40 km depth, compared with the three-layered crystalline crust on EEC detemined on a lot of seismic profiles acquired in 1960–1970 (Beloussov & Pavlenkova 1984; Pavlenkova 1996) and on LT-7 (Guterch *et al.* 1994), P4 profile (Grad *et al.* 2003) and CEL05 (Grad *et al.* 2006b), etc. The two layers (upper with velocities 6.23–6.35 km s^{-1} and lower with velocity ≈6.6 km s^{-1}) are separated by a smooth transition at a *ca.* 18 km depth. A fast velocity lower crust is absent; similar to modern and palaeo-extended continental regions (e.g. Western United States and Western Europe) and the similarity with the extended continental crust is further supported by a 28–30-km-thick basement.

Similar 40-km-thick crusts, with velocities ranging from 6.5 km s^{-1} at 6 km depth to 6.70 km s^{-1} at the Moho, was found in the Fore-Dobrudja Trough earlier, in the southernmost part of DOBRE-4 profile (Starostenko *et al.* 2013). The Fore-Dobrudja

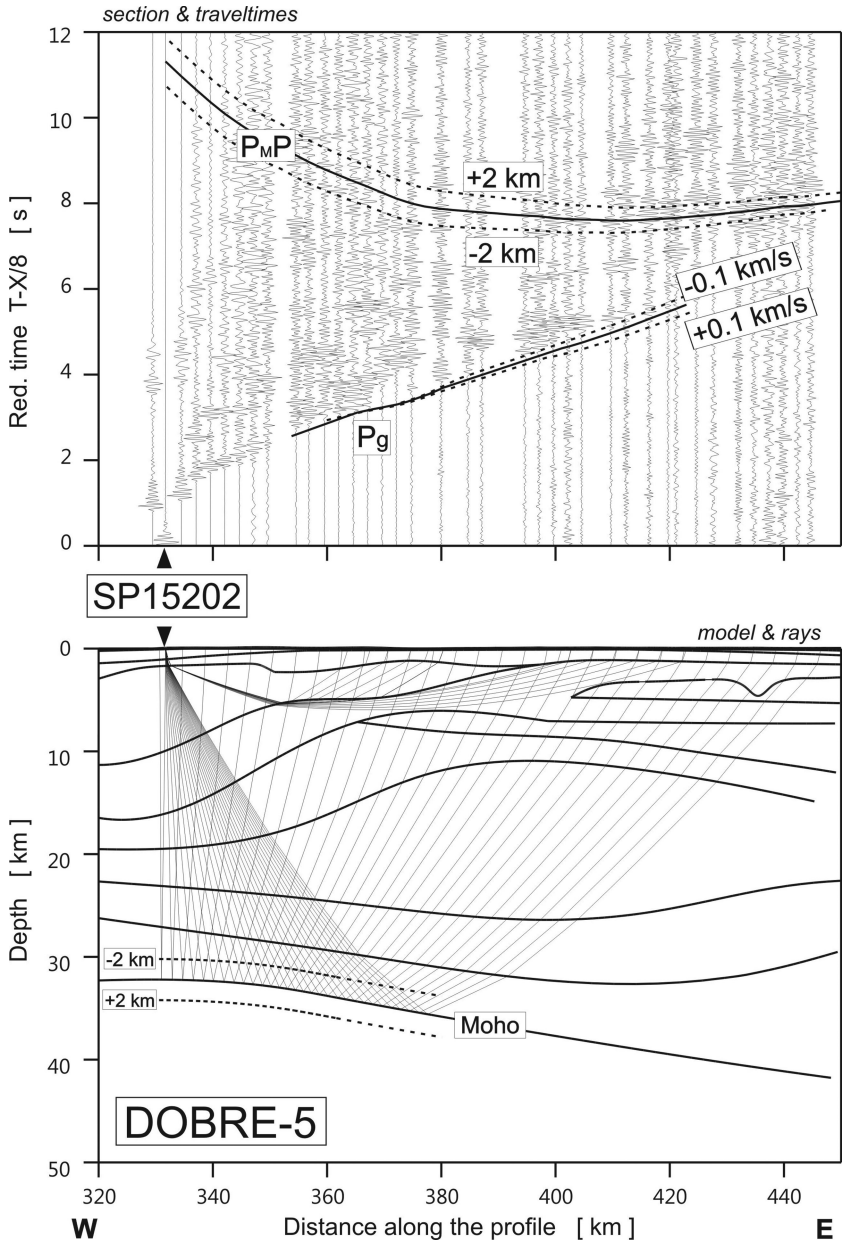

Figure 11. Seismic record section for SP15202 with P_g and P_MP traveltimes calculated for the final *P*-wave velocity model perturbed in one crustal layer (P_g) by ± 0.1 km s^{-1} as well as separately for the Moho depth (P_MP) by ± 2 km. Reduction velocity is 8 km s^{-1}.

Trough is considered as a foredeep of the North Dobrudja Orogen, which represents the TTZ in Romania (Khain 1977). The DOBRE-5 seismic model supports this view by revealing a crustal structure of the Fore-Dobrudja Trough which is similar to the TTZ and Western Europe, and is in a sharp contrast to the cratonic crust of the EEC (ScP) (Artemieva & Thybo 2013).

Along a fragment of the VRANCEA-2001 seismic line located in the North Dobrudja fold-thrust belt about 30 km from the SW end of the DOBRE-4 (Starostenko *et al.* 2013) and DOBRE-5 profiles (Fig. 1), the Moho boundary was modelled at a depth of 44 km (Hauser *et al.* 2007), that is 6 km deeper than in this and the DOBRE-4 profiles. Part of this difference may originate from the fact that the VRANCEA-2001 model is based on the assumption that the lower crustal velocities (6.7–7.1 km s^{-1}) are higher than along the DOBRE-5 profile.

6.3 The Karkinit Trough (km 160–380)

6.3.1 Sedimentary cover

A number of wells down to the depth of 4 km have been drilled on the Odessa Shelf (Denega *et al.* 1998; Khriachtchevskaia *et al.* 2010). The uppermost sedimentary sequences (700–800 m thick) with $V_p \approx 2.05$ km s^{-1} represents mainly shallow marine carbonate-terrigenous deposits of the middle Miocene–Quaternary above the clays of the Maikopian complex (Oligocene–Early Miocene) with $V_p = 2.24$ km s^{-1} (Fig. 5). The obtained velocities correspond with the velocities of 2.0–2.5 km s^{-1} determined for this complex within the Bulgarian shelf of the Black Sea (Finetti *et al.* 1998). The depths to the top (1.2–1.3 km) and base (~2 km) of the Maikopian complex in the Karkinit Trough (Fig. 5) are in agreement with the results of reflection and refraction studies in the northwestern

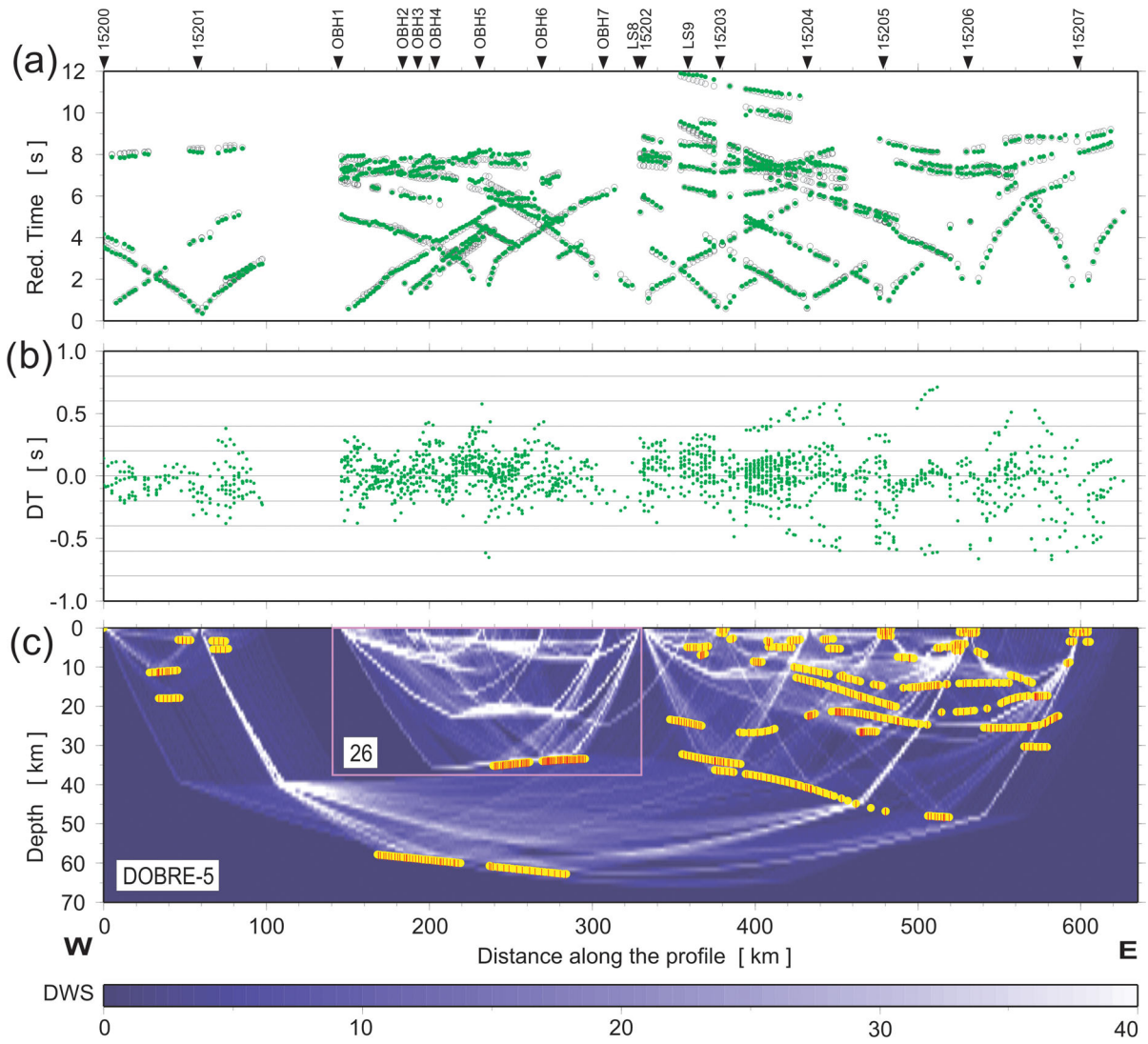

Figure 12. Calculated and observed traveltimes (a), traveltime residuals (b) and ray coverage (c) for all shot points an ocean bottom stations along profile DOBRE-5. Pink rectangle marks Profile-26. Green points – observed arrivals, black circles – theoretical traveltimes. Yellow lines – fragments of discontinuities constrained by reflected phases. The red points plotted on interfaces mark reflection points (every third point is plotted). Their density is a measure of the positioning accuracy of the reflectors. DWS, derivative weight sum. Reduction velocity is 8 km s^{-1}.

shelf of the Black Sea (Morgunov *et al.* 1981; Tugolesov *et al.* 1985; Sollogub *et al.* 1987; Khriachtchevskaia *et al.* 2010; Kozlenko *et al.* 2013).

The deeper, *ca.* 3 km and *ca.* 6–7 km thick, layers with velocities 3.0–4.0 and 5.55–5.70 km s^{-1} correspondingly are likely to be formed by Eocene–Upper Cretaceous limestone and marl and Lower Cretaceous clastic sedimentary sequences and volcanics (Plakhotny *et al.* 1971; Morgunov *et al.* 1981; Figs 5 and 13). The boundary between these layers corresponds approximately to the top of clastic and volcanic rocks of Cenomanian, in some places of Turonian age. Most probably, the Lower Cretaceous (Albian–Cenomanian) volcanic activity (Nikishin *et al.* 2001; Khriachtchevskaia *et al.* 2010) occurred in a marine environment, and at the final stage it developed into explosive volcanism which led to the formation of volcanic edifices and islands (one of them is at the Cape Tarkhankut at the westernmost part of the Crimea) (Figs 1 and 2). Some offshore wells have encountered andesites, andesitic tuffs and andesitic porfirite of Albian age (Nikishin *et al.* 2003 and references therein).

6.3.2 *Crystalline crust*

The folded basement of the Karkinit Trough may include Baikalian (Riphean–Cambrian), Variscan (Carboniferous–Lower Triassic) and Cimmerian (Middle Triassic–Lower Triassic) complexes (Muratov *et al.* 1968; Chekunov 1972; Morgunov *et al.* 1981; Kruglov & Tsypko 1988; Nikishin *et al.* 1998) without velocity discontinuities. The basement is formed chiefly by a 12-km-thick layer with V_p = 5.74–6.05 km s^{-1} (Fig. 5). The middle crustal layer is thin and probably does not exceed 3–5 in thickness. The Moho below the Karkinit Trough shallows from 38 km in the west to 33 km in the east below a high-velocity lower crust (HVLC) with V_p = 7.16 km s^{-1} (Fig. 5).

The HVLC is an asymmetric body with a maximal thickness of ~10 km at the western part of the trough (km 240), where the top of the HVLC shallows to ~21 km depth. It is constrained by reliable refractions and reflections from its top and bottom (the Moho). The HVLC may represent a part of the lower crust modified by magmatic or structural underplating or a mafic intrusion (*cf.* Lyngsie *et al.* 2007; Thybo & Artemieva 2013). The relatively

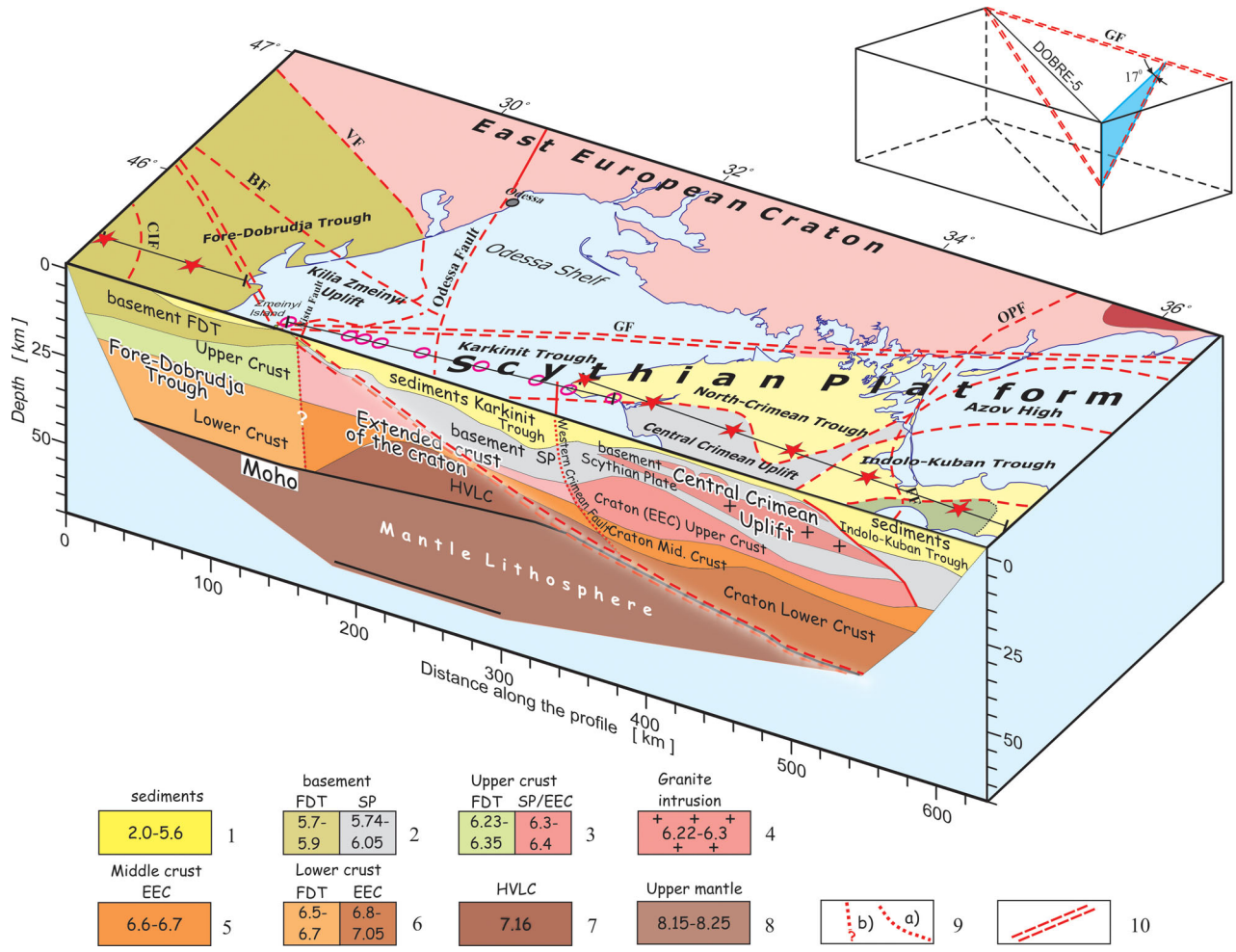

Figure 13. 3-D diagram combining the interpreted velocity model of the DOBRE-5 profile (Fig. 5) and surface geology (Fig. 2). Explanations in the text. For abbreviations see Fig. 2. Crustal units: 1 – sedimentary sequences with $V = 2.0$–$5.6\,km\,s^{-1}$; 2 – basement of the Fore-Dobrudja Trough (FDT) with $V_p = 5.7$–$5.9\,km\,s^{-1}$ and of the Scythian Platform (SP) with $V_p = 5.74$–$6.05\,km\,s^{-1}$; 3 – upper crust of the FDT with $V_p = 6.23$–$6.35\,km\,s^{-1}$ and of the SP/EEC with $V_p = 6.3$–$6.4\,km\,s^{-1}$; 4 – granitic intrusions in the basement of the ScP ($V_p = 6.22$–$6.3\,km\,s^{-1}$); middle crust of cratonic type, $V_p = 6.6$–$6.7\,km\,s^{-1}$; 5 – lower crust for the FDT ($V_p = 6.5$–$6.7\,km\,s^{-1}$) and for the EEC/SP (6.8–$7.1\,km\,s^{-1}$); high-velocity lower crust (HVLC) body below the Karkinit Trough ($V_p = 7.16\,km\,s^{-1}$); 8 – uppermost mantle with 8.15–$8.25\,km\,s^{-1}$ velocity; 9 – deep faults: (a) distinguished based on the changes of the seismic wavefield and related to the surface fault (Western Crimean Fault), (b) not clearly distinguished in the seismic section but related with surface (Nistru Fault) tectonics; 10 – red double dotted line indicates the crustal fault between the SP and EEC associated with the Golitsyn Fault (GF) on the surface. The inset diagram shows the 17° dipping angle between the EEC and the SP on the perpendicular slice to the GF.

high velocity ($7.16\,km\,s^{-1}$) of the HVLC and its sharp seismic boundaries could be indicative of a magmatic intrusion of mafic composition (gabbro, gabbro-norites and norites). However, the HVLC could also represent a continuation of the lower crust of the eastern ScP. It would then have been overthrust during collision and amalgamation, similar to observations in the North Sea (MONA LISA Working Group 1997; Abramovitz & Thybo 2000), the Baltic Sea (Thybo 2000) and in Poland (Jensen *et al.* 1999; Janik *et al.* 2002).

Since the DOBRE-5 profile runs across the Karkinit Trough, it is difficult to determine the geometry of the HVLC away from the profile. It may only relate to the lower crust of the Karkinit Trough, it could be a characteristic of the whole Odessa continental shelf, or it could represent an extension of the eastern ScP. Recent reinterpretation of existing DSS data of the N–S directed Profile-25 across the western Black Sea, and the E–W directed Profile-26 on the shelf (Fig. 1), include a 14-km-thick lower crustal layer below the Karkinit Trough with an internal velocity increase from 6.7 to $7.2\,km\,s^{-1}$ at the Moho at a depth of ~35 km (Yegorova *et al.* 2010; Baranova *et al.* 2011).

The gross features of the crustal structure of the Karkinit Trough are very similar to the Donbas segment of the Palaeozoic Dnieper-Donets rift basin at the southern margin of the EEC, where it is crossed by the DOBRE profile (DOBREfraction 99 Working Group 2003; Maystrenko *et al.* 2003), in particular regarding the configuration. However the HVLC below the sedimentary basin has slightly lower velocity and is less reflective than the body below the Donbas Rift. Nevertheless, we interpret the HVLC below the Karkinit Trough as the expression of mafic magmatic underplating or magmatic intrusion of mantle rocks into the lower crust during Cretaceous rifting. Similar interpretations have been made at presently active rift zones at Lake Baikal in Siberia (Thybo & Nielsen 2009), in Kenya and Ethiopia in eastern Africa (Thybo *et al.* 2000; Mackenzie *et al.* 2005) and in earlier extensional settings (Thybo & Schonharting 1991; Sandrin & Thybo 2008). Khriachtchevskaia *et al.* (2010) consider an Early Cretaceous (Aptian-Albian) age for the

active rifting stage at the Odessa Shelf that continued until the end of the Santonian in the Late Cretaceous. Similar evidence of rifting is found on Profile-25, which shows a normal fault at the edge of the continental margin of the EEC (ScP) that is interpreted as a first-order rift-controlling structure responsible for the opening of the West Black Sea Basin in the Cretaceous (Yegorova *et al.* 2010).

6.4 The Central Crimean Uplift (km 380–505)

6.4.1 Sedimentary cover

The central part of the Crimean Peninsula (the Crimean Plain and the Central Crimean Uplift) has a *ca.* 2–4-km-thick sedimentary cover with V_p = 2.70–3.0 km s^{-1} formed by Eocene–Upper Cretaceous limestones and marls, which are observed in boreholes on the Kerch Peninsula and exposed in the southwestern part of the Crimean Peninsula (the Cape Chauda) (Fig. 1). Several boreholes reach the basement. It consists of metamorphic rocks including mainly greenshists which were metamorphosed at 410–470 Ma (Belov 1981), as well as black shales, limestones and sandstones of Devonian and Carboniferous age (Zonenshain *et al.* 1990).

6.4.2 Crystalline crust

The heterogeneous basement of the Central Crimean Uplift thickens from 10 to 20 km from the western to the eastern part of the uplift. In general, the crustal structure of the Central Crimean Uplift is very similar to the crust of the EEC consisting of three layers with V_p = 5.8–6.4 km s^{-1} (upper crust), 6.5–6.6 km s^{-1} (middle crust) and 6.7–7.0 km s^{-1} (lower crust), which were determined for the EEC (Beloussov & Pavlenkova 1984; Pavlenkova 1996; Grad *et al.* 2006a,b; Janik *et al.* 2011, 2009a; Artemieva & Thybo 2013) and on the Baltic and Ukrainian Shields (BABEL Working Group 1993; Thybo 2000; Janik *et al.* 2007, 2009b; EUROBRIDGE'95 Seismic Working Group 2001).

The upper crustal layer with V_p = 5.74–6.0 km s^{-1} is *ca.* 8–15 km thick and, similar to the Karkinit Trough, may include the Baikalian, Variscan and Cimmerian basement. Three high-velocity bodies in the basement with V_p = 6.22–6.3 km s^{-1} (Fig. 5) (two small ones at a depth of ~5 km and one body at 10–15 km depth that extends across the whole uplift at profile distance km 360–560) are interpreted as granite intrusions. The age of these granites is generally accepted to be Late Palaeozoic (Khain 1977; Kruglov & Tsypko 1988; Zonenshain *et al.* 1990). Due to similarities in geology, composition and petrochemistry, the age may be close to 250–325 Ma as determined for magmatic rocks of the Fore-Caucasus (Belov 1981; Zakariadze *et al.* 2007; Adamia *et al.* 2011; Gamkrelidze *et al.* 2011; Rolland *et al.* 2011) and Dobrudja (Mutihac & Ionesi 1974). These rocks relate to a diorite-granodiorite formation associated with the orogenic stage of Variscan tectonic events (Khain 1977; Kruglov & Tsypko 1988). Similar granitic composition (granites, granodiorites and gneisses of different composition) is assumed for the upper part of the crystalline crust (V_p = 6.3–6.4 km s^{-1}) reaching 15 km in thickness in the eastern part of the uplift (Fig. 5). The thin (<5 km) middle crustal layer with a 6.6 km s^{-1} velocity, bounded by first order discontinuities in the mid-crustal interval, may be composed of diorites and enderbites (Christensen & Mooney 1995).

The lower crust of the Central Crimean Uplift with V_p = 6.8–7.0 km s^{-1}, thickens from 7 km in the west to 18 km in the east, in the area of the Indolo-Kuban Trough. The lower crust below the Central Crimean Uplift is characterized by a gradual westward velocity increase from 6.8 to 7.05 km s^{-1}, towards the HVLC below the Karkinit Trough. Hence, the lower crust of the Central Crimean Uplift might have another composition than the HVLC below the Karkinit Trough, perhaps mafic granulites, although they might also share the same origin as the HVLC. A similar thick high-velocity and density lower crust (of 6.8–7.1 km s^{-1} velocity and 3.06–3.10 g cm^{-3} density), represented by mafic granulites, was found in the southern part of the Ukrainian Shield along the southern part of the EUROBRIDGE-97 profile (Thybo *et al.* 2003; Yegorova *et al.* 2004).

An obtained velocity model of the Central Crimean Uplift along the DOBRE-5 profile (Fig. 13, between SP 15205 and 15206) shows good correspondence with the geotraverse III (Krasnopevtseva & Schukin 1993) in regards to *P*-wave velocities (6.3–6.4 km s^{-1}) in the upper crystalline crust down to a depth of 25 km. The high-velocity lower crust (7.0 km s^{-1}) occurred 30 km deeper in comparison with the lower crust velocities of 6.9–7.0 km s^{-1} on the DOBRE-5 profile. The Moho interface has been determined at a depth of 42–43 km on both profiles (Fig. 13; Krasnopevtseva & Schukin 1993). The velocity model of the crust of the Central Crimean Uplift might be interpreted as the thick Precambrian crust of the EEC with heterogeneous basement (greenschists and amphibolites) of the Baikalian–Variscan–(Cimmerian?) age. The basement and the uppermost crust underwent strong magmatic modifications in the Palaeozoic, evidenced by a number of inclusions of granitic bodies in the basement (Figs 5 and 13) which may have created the large uplift or dome of the Central Crimean Uplift. A similar interpretation (Khain 1977) has been proposed for other uplifts of the ScP (the Karabogaz and Central Karakum domes).

6.5 The Indolo-Kuban Trough (km 505–620)

6.5.1 Sedimentary cover

The easternmost part of the DOBRE-5 profile crosses the western part of the Indolo-Kuban Trough (km 505–620), which is conventionally related (together with the Terek-Caspian Trough) to the Greater Caucasus foredeep, that developed on the ScP basement. Along the profile, the Indolo-Kuban Trough is filled by up-to 10-km-thick sequence of sediments, mainly clay and molasse complexes of the Maikopian age (V_p = 2.70 km s^{-1}) and Eocene–Upper Cretaceous limestones and marls (V_p = 3.50–4.50 km s^{-1}). Approximately the same velocities (<3.0 and 4.0–4.2 km s^{-1}) were determined here at the depth of ~4 and >10 km correspondingly on the 28 profile at the crossing point with the DOBRE-5 line (Yegorova *et al.* 2010). Drill cores from borehole Gornostaevskaya-4 (GOR-4 in Fig. 5) in the Indolo-Kuban Trough indicate that the Palaeocene–Eocene formations constitute up to 30 per cent of the whole section of the layer. The Upper Cretaceous-Eocene sedimentary sequences with V_p ~ 4.5 km s^{-1} could have been thrust over the sequence with V_p = 3.50 km s^{-1}, and in that case they may be of an Upper Cretaceous to Eocene age.

The basin architecture of the Indolo-Kuban Trough (Fig. 5) correlates with the velocity structure of the sedimentary sequences on Profile-28 (Yegorova *et al.* 2010) and the DOBRE-2 profile (Starostenko *et al.* 2015), both crossing the trough in a N–S direction from the Azov Sea to the Black Sea (Fig. 1). Profile-28 shows sedimentary sequences with V_p < 3.0 km s^{-1} down to a depth of 3–3.4 km (3.5 km depth on DOBRE-5) and strata with velocities of 3.0–4.2 km s^{-1} down to 10.5 km depth as on the DOBRE-5 profile. In the DOBRE-2 seismic model, these two layers appear to extend

to 3.5 km ($V_p \geq 2.30\,km\,s^{-1}$) and 8 km ($V_p \approx 3.75\,km\,s^{-1}$) depth (Starostenko *et al.* 2015).

6.5.2 *Crystalline crust*

The uppermost crystalline crust ($V_p \approx 6.0\,km\,s^{-1}$) is *ca.* 12 km thick and extends down to a depth of ~22 km (Fig. 5). Below a *ca.* 25 km depth, the crustal structure of the Indolo-Kuban Trough is not resolved, because this is the easternmost part of the seismic profile, but the model indicates a structure similar to the Central Crimean Uplift (Fig. 5). The crust of the ScP below the Indolo-Kuban Trough, crossed by Profile-28, is interpreted to be cratonic (EEC; Yegorova *et al.* 2010). The mid crust velocities 6.3–6.5 $km\,s^{-1}$ here are very similar to that observed on the DOBRE-5 profile (Fig. 13). We observe no difference between the crustal structure of the ScP and the southern part of the EEC, which is consistent with models that explain the ScP as a reworked crust of the EEC during the Late Proterozoic and younger tectonism (Saintot *et al.* 2006).

6.6. Crust folding of the ScP along the DOBRE-5 profile

General bending and long-wavelength buckling of the ScP with a wavelength of ~230 km, observed throughout the crust (Fig. 5), could be a result of compressional deformation in the Crimean Mountains during the Alpine collisional tectonics. Lithosphere buckling and folding is thought to be an effective mechanism for the propagation of tectonic deformation from active plate boundaries far into intraplate domains (Stephenson & Cloetingh 1991; Burov *et al.* 1993; Ziegler *et al.* 1995). The wavelength of the lithosphere deformations/folding observed at different scales depends on thermotectonic age of the lithosphere, as well as its reological and thermal state. It is admitted the wavelength ~50–80 km for the crust folding and ~100–200 km (up to 300 km) for the lithospheric mantle (Cloetingh & Burov 2011).

Alpine compressional tectonics was the principal factor for the lithospheric folding of Iberia, Pannonian Basin, South-Caspian Basin, Black Sea Basin (Cloetingh *et al.* 2002, 2008; Guest *et al.* 2007; Matenco *et al.* 2007). European Alpine foreland lithosphere experienced also large scale compressional deformations. Lithospheric scale folding in the Early Cretaceous–Early Cenozoic was found for the North-German Basin (Marotta *et al.* 2000). Cenozoic deformations are thought to be responsible for the lithosphere folding of the North Sea Basin (Scheck & Bayer 1999) and contribute to the long-wavelength folding of the Paris Basin lithosphere (Bourgeois *et al.* 2007).

Comprehensive review papers considering complex thermomechanical aspects of lithosphere-scale folding, its topographic effects and influence on sedimentary basin formation and evolution were published by Cloetingh *et al.* (1999) and by Cloetingh & Burov (2011). Most of the outcomes from the lithosphere or crustal folding have been based on an interpretation of topographic elevations and depressions and their reflections in geological maps or in reflection seismics. Very few examples of the crust/upper mantle folding are known from deep refraction/reflection seismics. One of them is the spectacular Moho folds, associated with the folding of cold lithosphere with a relatively strong mantle, with the wavelength of the order of 150 km and the amplitude attaining 8–17 km revealed in the southern margin of the EEC on the DOBRE-4 deep seismic (WARR) profile (Starostenko *et al.* 2013). The undulations in the crust and upper mantle are explained by compressional lithospheric scale buckling as a result of Late Jurassic–Early Cretaceous and/or end Cretaceous collision related tectonic events, associated with the closure of the Palaeotethys and Neotethys oceans (Starostenko *et al.* 2013). That corresponds with the crust and Moho folding with a wavelength of the order ~230 km revealed on the DOBRE-5 profile (Fig. 13) and could suggest it originating within the lithosphere of the southern margin (southernmost part) of the EEC (ScP) affected by Alpine collision.

Another important aspect of the lithosphere (crust) folding is its linkage to brittle deformations and faulting. The surface expression of folding in uniform lithosphere is frequently in the form of fault-controlled pop-up and pop-down structures and inverted basins (Cobbold *et al.* 1993; Sokoutis *et al.* 2005). Crustal and mantle faults may develop as a result of folding; folding can contribute after these faults develop and folding and faulting can co-exist for times of several Myr (Burov & Molnar 1998). That corresponds with our findings on the lithosphere folding of the ScP on the DOBRE-5 line, which is bounded from the EEC by a crustal fault deeping southward below the ScP at a low angle (Fig. 13).

6.7 Faults in the ScP along the DOBRE-5 profile

A number of faults separate crustal blocks in the ScP (Fig. 2), and many of them have an approximately NW–SE orientation. The Fore-Dobrudja Domain terminates to the east at the NS trending Nistru fault (Morosanu 2007). The Western Crimean Fault separates the Karkinit Trough and the Central Crimean Uplift; the latter is separated from the Indolo-Kuban Trough by the Feodosiya Fault—the southern continuation of the Proterozoic Orekhovo-Pavlograd fault of the Ukrainian Shield (Fig. 2). Two SW–NE oriented faults, the Golitsyn and Azov faults may mark the transition from the EEC to the ScP.

The Golitsyn fault (Figs 2 and 13) runs across the Odessa Shelf and outcrops at the surface at the Zmeinyi Island near the Kiliya-Zmeinyi Uplift (km 150), at the offshore continuation of the Fore-Dobrudja Trough. This fault may be traced at depth along the western flank of the basement depression of the Karkint Trough (down to ~12 km depth) and in the lower crust—along the refraction-reflection boundary on the eastern slope of the HVLC below the Karkinit Trough (Figs 5 and 13). It may continue further eastwards along the Moho that deepens from 32 km below the Karkinit Trough to 47 km at the eastern termination of the Central Crimean Uplift (km 520) over a total distance of ~370 km along the DOBRE-5 profile. The fault outcrops at the surface near the Zmeinyi Island, close to the sublatitudinal southern margin of the EEC and to the sublongitudinal Nistru Fault (Figs 2 and 13). This leaves two possibilities for the interpretation of the origin of this crustal fault. The fault may be associated with extensional tectonics (rifting) along the southern margin of the EEC (ScP). In this case, the HVLC below the Karkinit Trough may be caused by magmatic underplating if the extension along the southern margin of the EEC was longitudinal. This W–E-oriented crustal fault may represent the crustal divider between the crust of the EEC to the north and the reworked crust of the SCP to the south (its projection on the surface is shown by a double dotted red line in Fig. 2). The surface expression of the deep fault is the Golitsyn Fault, which is observed at the surface between the EEC and the ScP (Fig. 2). Since the DOBRE-5 profile is subparallel to this boundary, the velocity cross-section (Fig. 5) shows the projection at an angle of ~17° (Fig. 13).

Another interpretation assumes an alternative, sublongitudinal orientation of this crustal fault - across the DOBRE-5 profile. In this case it could be associated with the Nistru Fault (Fig. 2) that

comes at the surface at the Kiliya-Zmeinyi Uplift, located between the Fore-Dobrudja Domain and the Karkinit Trough (Figs 5 and 13). This interpretation assumes sublatitudinal extension in the Karkinit Trough. It is difficult to explain the origin of the oval-shaped sublatitudinal West Black Sea Basin by sublatitudinal extension, but such a possibility has been argued in some interpretations of the opening of the East Black Sea Basin (Okay *et al.* 1994; Finetti *et al.* 1998; Shillington *et al.* 2009).

The Western Crimean Fault may be associated with the transition between the two domains of the ScP (the offshore Karkinit Trough and the onshore Central Crimean Uplift) in the central part of the DOBRE-5 profile. The Western Crimean Fault together with the Odessa Fault (Fig. 2) constitutes a system of major N–S-oriented faults on the Odessa Shelf. Further, the seismic model (Fig. 5) may show evidence for the Feodosiya fault (down to the depth of ∼23 km), between the Indolo-Kuban Trough and the Central Crimean Uplift. This fault has been observed in the sedimentary sequences and in the basement of the Indolo-Kuban Trough down to a depth of ∼23 km. It could be the southern continuation of a Proterozoic fault zone (Orekhovo-Pavlograd Fault), observed in the Ukrainian Shield (Fig. 2; Sollogub 1986), that has been reactivated during Palaeozoic–Mesozoic tectonic events.

7 CONCLUSIONS

The WARR seismic model along the sublatitudinal DOBRE-5 profile provides new constraints on the crustal structure of the ScP, between the Precambrian EEC in the north and the Crimean-Caucasus orogenic belt and Black Sea Basin in the south. By the structure of the crust we recognize from west to east four characteristic crustal domains, which may be separated by faults. They represent the Fore-Dobrudja Domain and three domains in the ScP including the offshore block of the Karkinit Trough at the Odessa Shelf of the Black Sea, the onshore domain of the Central Crimean Uplift at Crimean Plain (Crimean Peninsula) and the Indolo-Kuban Trough at the Kerch Peninsula.

(1) The Fore-Dobrudja Trough has a 10–12-km-thick sedimentary cover which includes an 8–10-km-thick layer with $V_p \sim 5.7$–$5.8\,\mathrm{km\,s^{-1}}$ and a two-layered crystalline crust where the lower crust is absent. The structure of the crust indicates a different affinity than the EEC. This crustal type is similar to that of the Trans-European Suture Zone and the Variscan Western Europe, although the crust is thicker with the Moho at a 38–40 km depth.

(2) The offshore Karkinit Trough of the Odessa Shelf has a 6–11 km thick sedimentary cover, with *ca.* 4 km of low-V_p (2.0–$4.0\,\mathrm{km\,s^{-1}}$) sediments, which thickens to the east due to an increase of fast-velocity (5.6–$5.7\,\mathrm{km\,s^{-1}}$) sediments from 2 to 7 km at the western coast of Crimea, a 12-km-thick upper crust, and 3–5-km-thick middle crustal layer. The Moho shallows eastwards from 38 to 33 km. A high-velocity lower crust (HVLC) with a maximal thickness of ∼10 km at the western part of the trough is interpreted as mafic magmatic underplating (or intrusion) during Cretaceous rifting, contemporaneous with volcanic activity in the Karkinit Trough. The transition between the offshore Karkinit Trough and the onshore Central Crimean Uplift is marked by the sublongitudinal Western Crimean Fault, which separates the regions affected by Cretaceous extension/rifting (the Odessa Shelf) and on-going compressional tectonics in Crimea (Fig. 13).

(3) The Central Crimean Uplift has a *ca.* 2–4-km-thick sedimentary cover ($V_p \sim 2.70$–$3.0\,\mathrm{km\,s^{-1}}$) atop heterogeneous basement which thickens eastwards from 10 to 20 km. Three high-velocity bodies ($V_p = 6.22$–$6.3\,\mathrm{km\,s^{-1}}$) within an 8–16-km-thick upper crustal layer (heterogeneous basement formed during the Variscan, Cimmerian and Alpine tectogenesis) are interpreted as granite intrusions emplaced during the Variscan orogeny. The crust is thick (up to 47 km), and similarity of the velocity structure of the crust to the cratonic three-layer crust of the EEC suggests that the ScP formed on the crust of the Precambrian craton (EEC).

(4) The Indolo-Kuban Trough has an up-to 10-km-thick sequence of low-V_p sediments, and a *ca.* 12-km-thick upper crust, with the velocity model not resolved below a *ca.* 25 km depth, although data from the crossing Profile-28 suggests it may be a reworked cratonic crust of the EEC.

(5) General bending and crust scale buckling of the ScP with the wavelength of ∼230 km could be an effect of the Alpine compressional tectonics in the Crimean Mountains. The result of this folding could be seen in the crustal fault of ∼W–E orientation, which separates the southern margin of the EEC from the ScP and corresponds with the Golitsyn Fault observed at the surface between the EEC and ScP.

ACKNOWLEDGEMENTS

The DOBRE-5 profile was acquired through an international collaboration between institutions and organisations from Ukraine (Institute of Geophysics, National Academy of Sciences of Ukraine, and the State Geophysical Enterprise ‘Ukrgeofizika’, Kiev), Denmark (Geology Section, IGN, University of Copenhagen), Finland (Institute of Seismology, University of Helsinki) and Poland (Institute of Geophysics, Polish Academy of Sciences). Participation of the Polish group in this work was supported within statutory activities No 3841/E-41/S/2014 of the Ministry of Science and Higher Education of Poland. Participation of scientists from the University of Sophia Antipolis (Nice, France) facilitates geological investigation in Crimea. The authors express their sincere appreciation of the activities by the many people who took part in field work and data acquisition. The authors are grateful to the Geophysical Journal International editor Prof Randy Keller (University of Oklahoma, USA) and three rewievers: Prof Nina Pavlenkova (Institute of the Physics of the Earth, RAS, Moscow, Russia), Prof Sierd Cloetingh (Utrecht University, Utrecht, Netherlands) and an anonymous reviewer for helpful comments and suggestions. The public domain GMT package (Wessel & Smith 1995) was used to produce some of the maps.

REFERENCES

Abramovitz, T. & Thybo, H., 2000. Seismic images of Caledonian, lithosphere-scale collision structures in the southeastern North Sea along MONA LISA Profile 2, *Tectonophysics,* **317,** 27–54.

Adamia, Sh., Zakariadze, G., Chkhotua, T., Sadradze, N., Tsereteli, N., Chabukiani, A. & Gventsadze, A., 2011. Geology of the Caucasus: a review, *Turkish J. Earth Sci.,* **20,** 489–544.

Aichroth, B., Prodehl, C. & Thybo, H., 1992. Crustal structure along the central segment of the EGT from seismic-refraction studies, *Tectonophysics,* **207,** 43–64.

Artemieva, I.M., 2011. *The Lithosphere: An Interdisciplinary Approach,* Cambridge Univ. Press, Monograph, 794 pp.

Artemieva, I.M. & Meissner, R., 2012. Crustal thickness controlled by plate tectonics: a review of crust–mantle interaction processes illustrated by European examples, *Tectonophysics,* **519,** 3–34.

Artemieva, I.M. & Thybo, H., 2013. EUNAseis: a seismic model for Moho and crustal structure in Europe, Greenland, and the North Atlantic region, *Tectonophysics,* **609,** 97–153.

BABEL Working Group, 1993. Deep seismic reflection/refraction interpretation of crustal structure along BABEL profiles A and B in the southern Baltic Sea, *Geophys. J. Int.,* **112,** 325–343.

Balintoni, I., Balica, C., Seghedi, A. & Ducea, M.N., 2010. Avalonian and Cadomian terranes in North Dobrogea, Romania, *Precambrian Res.,* **182,** 217–229.

Baranova, E.P., Yegorova, T.P. & Omelchenko, V.D., 2011. Detecting wave guides in the basement of the North West Shelf of the Black Sea by the results of reinterpretation of the DSS materials of 26th and 25th profiles, *Geophys. J.,* **6,** 15–29 (in Russian).

Beloussov, V.V. & Pavlenkova, N.I., 1984. Types of the Earth's crust, *J. Geodyn.,* **1,** 167–183.

Beloussov, V.V. & Volvovsky, B.S. (eds), 1989. *Structure and Evolution of the Earth's Crust and Upper Mantle of the Black Sea,* Nauka, 207 pp. (in Russian).

Belov, A.A., 1981. *Tectonic Development of the Alpine Folded Zone in the Paleozoic,* Nauka, 212 pp. (in Russian).

Bourgeois, O., Ford, M., Diraison, M., Le Carlier de Veslud, C., Gerbault, M., Pik, R., Ruby, N. & Bonnet, S., 2007. Separation of rifting and lithospheric folding signatures in the NW-Alpine foreland, *Int. J. Earth Sci.,* **96,** 1003–1031.

Burov, E., Lobkovsky, L., Cloetingh, S. & Nikishin, A., 1993. Continental lithosphere folding in Central Asia. Part 2: constraints from gravity and topography, *Tectonophysics,* **226,** 73–87.

Burov, E.B. & Molnar, P., 1998. Gravity anomalies over the Ferghana Valley (central Asia) and intracontinental deformation, *J. geophys. Res.,* **103,** 18 137–18 152.

Červený, V. & Pšenčík, I., 1984. SEIS83—numerical modelling of seismic wave fields in 2-D laterally varying layered structures by the ray method, in *Documentation of Earthquake Algorithms,* pp. 36–40, ed. Engdahl, Rep. SE-35, World Data Center (A) for Solid Earth Geophysics.

Chekunov, A.V., 1972. *Structure of the Earth Crust and Tectonics of the Europeian Part of the USSR,* Naukova Dumka, 176 pp. (in Russian).

Chekunov, A.V. (ed.), 1994. *The Lithosphere of the Central and Eastern Europe—Young Platforms and the Alpine Fold Belt,* Naukova dumka, 331 pp. (in Russian).

Christensen, N.I. & Mooney, W.D., 1995. Seismic velocity structure and composition of the continental crust: a global view, *J. geophys. Res.,* **100,** 9761–9788.

Cloetingh, S. & Burov, E.B., 2011. Lithospheric folding and sedimentary basin evolution: a review and analysis of formation mechanisms, *Basin Res.,* **23,** 257–290.

Cloetingh, S., Burov, E. & Poliakov, A., 1999. Lithosphere folding: primary response to compression? (from Central Asia to Paris Basin), *Tectonics,* **18,** 1064–1083.

Cloetingh, S., Burov, E., Beekman, F., Andriessen, P.A.M., Garcia-Castellanos, D., De Vicente, G. & Vegas, R., 2002. Lithospheric folding in Iberia, *Tectonics,* **21,** 1041.

Cloetingh, S., Beekman, F., Van Wees, J.D., Ziegler, P.A. & Sokoutis, D., 2008. Post-rift compressional reactivation potential of passive margins and extensional basins, in *Compressional Deformation within Passive Margins: Nature, Causes and Effects,* Vol. 306, pp. 27–70, eds Johnson, H. *et al.,* Geol. Soc. Lond. Spec. Publ.

Cobbold, P.P., Davy, D., Gapais, E.A., Rossello, E., Sadybakasov, J.C., Thomas, J.J., Tondji, B. & De Urreiztieta, M., 1993. Sedimentary basins and crustal shortening, *Sediment. Geol.,* **86,** 77–89.

Denega, B.I., Nimets, M.V., Pavlyuk, M.I., Palinsky, R.V., Polukhtovych, B.M. & Fedyshyn, V.O. (eds), 1998. Southern oil-and gas bearing region, in *Atlas Oil and Gas Fields of Ukraine,* six volumes, Ukrainian Oil and Gas Academy, 4–41 pp. (in Ukrainian).

Dinu, C., Wong, H.K. & Ţambrea, D., 2002. Stratigraphic and tectonic syntheses of the Romanian Black Sea shelf and correlation with major land structures, *Bucharest Geoscience Forum,* **2,** 101–117.

Dinu, C., Wong, H.K., Tambrea, D. & Matenco, L., 2005. Stratigraphic and structural characteristics of the Romanian Black Sea shelf, *Tectonophysics,* **410,** 417–435.

DOBREfraction'99 Working Group, 2003. "DOBREfraction'99"—velocity model of the crust and upper mantle beneth the Donbas Foldbelt (East Ukraine), *Tectonophysics,* **371,** 81–110.

Ermakov, Yu.G., Kirikilitsa, S.I., Volfman, Yu.M. & Shcherbakov, L.N., 1985. Structural forms of Vendian-Early Mesozoic tectonic activity of the Transnistrian Russian Plate, *Geol. J.,* **45**(4), 117–127 (in Russian).

Ermakov, Yu.G. & Volfman, Yu.M., 1986. Extensional rifting and its role in the formation of platform structures foreland of uplifts of Dobrudja and Crimean Mountains, *Rep. Ukrainian Acad. Sci.,* **4,** 9–12 (in Russian).

EUROBRIDGE'95 Seismic Working Group, 2001. EUROBRIDGE'95: deep seismic profiling within the East European Craton, *Tectonophysics,* **339,** 153–175.

Finetti, I., Bricchi, G., Del Ben, A., Pipan, M. & Xuan, Z., 1998. Geophysical study of the Black Sea, *Bolletino di Geofisica Teorica ed Applicata,* **XXX/811-711,** 423–791.

Galetsky, L.S. (ed.), 2007. *An Atlas of the Geology and Mineral Deposits of Ukraine,* University of Toronto Press, 168 pp.

Gamkrelidze, I., Shengelia, D., Tsutsunava, T., Chung, S-L., Chiu, H-Y. & Chikhelidze, K., 2011. New data on the U-Pb zircon age of the pre-Aipine crystalline basement of the Black Sea—Central Transcaucasian Terrane and their geological significance, *Bull. Georgian Natl. Acad. Sci.,* **5**(1), 64–75.

Gazizova, S.A., 2009. Towards a comparative analysis of basins surrounding the East-European Platform. The Dobrudja Foredeep Basin, *Geologicheskiy sbornik Instituta Geologii Ufimskogo Nauchnogo Centra Rossiyskoy Akademii Nauk,* **8,** 88–93 (in Russian).

Gee, D. & Stephenson, R.A. (eds), 2006. *European Lithosphere Dynamics*. Geological Society, Memoir 32, 662 pp.

Gobarenko, V.S. & Yanovskaya, T.B., 2011. Velocity structure of the upper stages of the mantle under the Black Sea, *Geophys. J.,* **3,** 62–74 (in Russian).

Gobarenko, V.S., Yegorova, T.P. & Stephenson, R.A., 2015. Local tomography model of the northeast Black Sea: intraplate crustal underthrusting, *Geol. Soc., Spec. Publ.,* in press.

Grad, M. *et al.*, 2003. Crustal structure of the Trans-European suture zone region along POLONAISE'97 seismic profile P4, *J. geophys. Res.,* **108**(B11), doi:10.1029/2003JB002426.

Grad, M. *et al.*, 2006a. Lithospheric structure beneath trans-Carpathian transect from Precambrian platform to Pannonian basin: CELEBRATION 2000 seismic profile CEL05, *J. geophys. Res.,* **111,** B03301, doi:10.1029/2005JB003647.

Grad, M., Janik, T., Guterch, A., Środa, P. & Czuba, W. EUROBRIDGE'94-97, POLONAISE'97 & CELEBRATION 2000 SeismicWorking Groups, 2006b. Lithospheric structure of the western part of the East European Craton investigated by deep seismic profiles, *Geol. Quart.,* **50**(1), 9–22.

Guest, B., Guest, A. & Axen, G., 2007. LateTertiary tectonic evolution of northern Iran: a case for simple crustal folding, *Global Planet. Change,* **58,** 435–453.

Guterch, A. *et al.*, 1994. Crustal structure of the transitional zone between Precambrian and Variscan Europe from new seismic data along LT-7 profile (NW Poland and eastern Germany), *C. R. Acad. Sc. Paris,* II, **319**(2), 1489–1496.

Hauser, F., Raileanu, V., Fielitz, W., Dinu, C., Landesa, M., Bala, A. & Prodehl, C., 2007. Seismic crustal structure between the Transylvanian Basin and the Black Sea, Romania, *Tectonophysics,* **430,** 1–25.

Hippolyte, J.C., 2002. Geodynamics of Dobrogea (Romania): new constraints on the evolution of the Tornquist-Teisseyre Line, the Black Sea and the Carpathians, *Tectonophysics,* **357,** 33–53.

Ivanova, A.V., 2011. Catagenesis of Phanerozoic rocks of the area between the Dnieper and Prut as a result of pecularities of its geological evolution, *Dopovidy Nacionalnoy Akademii Nauk Ukrainy,* **1,** 91–97 (in Russian).

Janik, T., Yliniemi, J., Grad, M., Thybo, H. & Tiira, T. POLONAISE P2 Working Group, 2002. Crustal structure across the TESZ along POLONAISE'97 seismic profile P2 in NW Poland, *Tectonophysics,* **360,** 129–152.

Janik, T., Kozlovskaya, E. & Yliniemi, J., 2007. Crust-mantle boundary in the central Fennoscandian shield: Constraints from wide-angle *P* and *S* wave velocity models and new results of reflection profiling in Finland, *J. geophys. Res.,* **112,** B04302, doi:10.1029/2006JB004681.

Janik, T., Grad, M. & Guterch, A. CELEBRATION 2000 Working Group, 2009a. Seismic structure of the lithosphere between the East European

Craton and the Carpathians from the net of CELEBRATION 2000 profiles in SE Poland, *Geol. Quart.,* **53**(1), 141–158.

Janik, T., Kozlovskaya, E., Heikkinen, P., Yliniemi, Ju. & Silvennoinen, H., 2009b. Evidence for preservation of crustal root beneath the Proterozoic Lapland-Kola orogen (northern Fennoscandian shield) derived from *P* and *S* wave velocity models of POLAR and HUKKA wide-angle reflection and refraction profiles and FIRE4 reflection transect, *J. geophys. Res.,* **114,** B06308, doi:10.1029/2008JB005689.

Janik, T. *et al.*, 2011. Crustal structure of the Western Carpathians and Pannonian Basin: seismic models from CELEBRATION 2000 data and geological implications, *J. Geodyn.,* **52,** 97–113.

Jensen, S.L., Janik, T. & Thybo, H., 1999. Seismic structure of the Palaeozoic Platform along POLONAISE'97 profile P1 in northwestern Poland, *Tectonophysics,* **314,** 123–143.

Jensen, S.L. & Thybo, H. Polonaise'97 Working Group, 2002. Moho topography and lower crustal wide-angle reflectivity around the TESZ in southern Scandinavia and northeastern Europe, *Tectonophysics,* **360,** 187–213.

Khain, V.E., 1977. *Regional Geotectonics. Europe Outside the Alps and Western Asia,* Nedra, 359 pp. (in Russian).

Khomenko, V.I., 1987. *Deep Structure of the South-Western Edge of the East-European Platform* Naukova Dumka, 140 pp. (in Russian).

Khriachtchevskaia, O., Stovba, S. & Stephenson, R., 2010. Cretaceous-Neogene tectonic evolution of the northen margin of the Black Sea from seismic reflection data and tectonic subsidence analysis, in *Sedimentary Basin Tectonics from the Black Sea and Caucasus to the Arabian Platform,* Vol. 340, pp. 137–157, eds Sosson, M., Kaymakci, N., Stephenson, R.A., Bergerat, F. & Starostenko, V., Geological Society, Special Publications.

Komminaho, K., 1998. *Software Manual for Programs MODEL and XRAYS: A Graphical Interface for SEIS83 Program Package,* Vol. 20, University of Oulu, Dep. of Geophys., Rep, 31 pp.

Kozlenko, M.V., Kozlenko, Ju.V. & Lysynchuk, D.V., 2013. The structure of the Earth's crust of the north-western shelf of the Black Sea along the profile 25, *Geophys. J.,* **1,** 158–168 (in Russian).

Krasnopevtseva, G.V. & Schukin, Yu.K., 1993. Lithosphere structure along the geotraverse III, in *Lithosphere of Central and East Europe. Geotraverse III, VI, IX,* Naukova Dumka, 8–77 pp. (in Russian).

Kruglov, S.S., 2001. *The Problems of Tectonics and Paleogeodynamics of Western Ukraine* (A critical survey of new publications), pp. 83, Interdepartmental Tectonic Committee of Ukraine (in Ukrainian).

Kruglov, S.S. & Tsypko, A.K (eds.), 1988. *Tectonic of Ukraine,* Nedra, 254 pp. (in Russian).

Lyngsie, S.B., Thybo, H. & Lang, R., 2007. Rifting and lower crustal reflectivity: a case study of the intracratonic Dniepr-Donets rift zone, Ukraine, *J. geophys. Res.,* **112**(1–27), B12402, doi:12410.11029/12006JB004795.

Mackenzie, G.D., Thybo, H. & Maguire, P.K.H., 2005. Crustal velocity structure across the Main Ethiopian Rift: results from two-dimensional wide-angle seismic modelling, *Geophys. J. Int.,* **162,** 994–1006.

Malovitskiy, Ya.P. & Neprochnov, Yu.P. (eds.), 1972. *Structure of the Western Part of the Black Sea Basin Nauka,* 243 pp., (in Russian).

Marotta, A.M., Bayer, U. & Thybo, H., 2000. The legacy of the NE German Basin - reactivation by compressional buckling, *Terra Nova,* **12,** 132–140.

Marotta, A.M., Bayer, U., Thybo, H. & Scheck, M., 2002. Origin of the regional stress in the North German basin: results from numerical modelling, *Tectonophysics,* **360,** 245–264.

Matenco, L., Bertotti, G., Leever, K., Cloetingh, S., Schmid, S., Tărăpoancă, M. & Dinu, C., 2007. Large-scale deformation in a locked collisional boundary: interplay between subsidence and uplift, intraplate stress, and inherited lithospheric structure in the late stage of the SE Carpathians evolution, *Tectonics,* **26,** 1–29.

Maystrenko, Yu. *et al.*, 2003. Crustal-scale pop-up structure in cratonic lithosphere: DOBRE seismic reflection study of the Donbas fold belt, Ukraine, *Geology,* **31,** 733–736.

Meissner, R., 1986. *The Continental Crust: a Geophysical Approach,* Academic Press, 426 pp.

Milanovsky, E.E., 1991. *Geology of the USSR,* Part 3, University Press, 273 pp. (in Russian).

Milanovsky, E.E., 1996. *Geology of Russia and Adjacent Areas (Northern Eurasia),* University Press, 448 pp. (in Russian).

MONA LISA Working Group, 1997. Closure of the Tornquist sea: Constraints from MONA LISA deep seismic reflection data, *Geology,* **25,** 1071–1074.

Morgunov, Yu.G, Kalinin, A.V., Kalinin, V.V., Kuprin, P.N., Limonov, A.F., Pivovarov, B.L. & Shcherbakov, F.A. (eds), 1981. *Tectonic and Evolution of the North-Western Shelf of the Black Sea,* Nauka, 244 pp. (in Russian).

Morosanu, I., 2007. *Romanian Continental Plateau of the Black Sea,* Oscar Print, 176 pp.

Moskalenko, V.N. & Malovitsky, Y.P., 1974. Results of deep seismic sounding along the transmeridional profile across the Azov and Black Seas. *Izvestiya of Academy of Sciences of the USSR*, *Ser. Geol.,* **9,** 23–31 (in Russian).

Munteanu, I., Matenco, L., Dinu, C. & Cloetingh, S., 2011. Kinematics of back-arc inversion of the Western Black Sea Basin, *Tectonics,* **30,** 1–21, doi:10.1029/2011TC002865.

Munteanu, I., Willingshofer, E., Sokoutis, D. & Matenco, L., 2013. Transfer of deformation in back-arc basins with a laterally variable rheology: Constraints from analogue modelling of the Balkanides-Western Black Sea inversion, *Tectonophysics,* **602,** 223–236.

Muratov, M.V. (ed.), 1969. *Geology of the USSR,* Vol. VIII, The Crimea: Part 1, Geological Description, Nedra, 575 pp. (in Russian).

Muratov, M.V., Bondarenko, V.G. & Plakhotny, L.G., 1968. The structure of the folded base plain Crimea, *Geotectonics,* **4,** 54–70 (in Russian).

Mutihac, V. & Ionesi, L., 1974. *Geologia Romaniei,* Editura Tehnicâ, 648 pp. (in Romanian).

Natal'in, B.A. & Şengör, A.M.C., 2005. Late Palaeozoic to Triassic evolution of the Turan and Scythian platforms: the pre-history of the Palaeo-Tethyan closure, *Tectonophysics,* **404,** 175–202.

Neprochnov, Y.P., Kosminskaya, I.P. & Malovitsky, Y.P., 1970. Structure of the crust and upper mantle of the Black and Caspian Seas, *Tectonophysics,* **10,** 517–538.

Nikishin, A.M., 2001. Mesozoic and Cenozoic evolution of the Scythian Platform-Black Sea-Caucasus domain, in *Peri-Tethys Memoir 6. Peri Tethyan Rift / Wrench Basins and Passive Margins,* Vol. 186, pp. 296–346, eds Ziegler, P.A., Cavazza, W., Robertson, A.H.F. & Crasquin-Solau, S. *et al.*, Mémoires du Musée National d'Histoire Naturelle.

Nikishin, A. M., Ziegler, P., Bolotov, S. & Fokin, P., 2011. Late Palaeozoic to Cenozoic Evolution of the Black Sea-Southern Eastern Europe Region: a view from the Russian Platform, *Turkish J. Earth Sci.,* **20,** 571–634.

Nikishin, A.M., Cloetingh, S., Brunet, M.F., Stephenson, R.A., Bolotov, S.N. & Ershov, A.V., 1998. Scythian Platform, Caucasus and Black Sea region: Mesozoic-Cainozoic evolution tectonic and dynamics, in *Peri-Tethys Memoir 3: Stratigraphy and evolution of Peri-Tethys Platforms,* pp. 163–176, eds Crasquin-Soleau, S. & Darrier, E., Mémoires du Musée National d'Histoire Naturelle.

Nikishin, A.M., Korotaev, M.V., Ershov, A.V. & Brunet, M.F., 2003. The Black Sea Basin: tectonic history and Neogene–Quaternary rapid subsidence modelling, *Sedimentary Geology,* **156,** 149–168.

Okay, A.I. & Tüysüz, O., 1999. Tethyan sutures of northern Turkey, in *The Mediterranean Basins: Tertiary Extension within the Alpine Orogen,* Vol. 156, pp. 475–615, eds Durand, B., Jolivet, L., Horváth, F. & Séranne, M., Geological Society, Special Publications.

Okay, A.I., Şengör, A.M.C. & Görür, N., 1994. Kinematic history of the opening of the Black Sea and its effect on the surrounding regions, *Geology,* **22,** 267–270.

Okay, A.I., Satir, M., Maluski, H., Siyako, M., Monie, P., Metzger, R. & Akyüz, S., 1996. Paleo- and Neo-Tethyan events in northwest Turkey: geological and geochronological constraints, in *Tectonics of Asia,* pp. 420–441, eds Yin, A. & Harrison, M., Cambridge University Press.

Papanikolaou, D., Barghathi, H., Dabovski, Ch., Dimitriu, R., El-Hawat, A., Ioane, D., Seghedi, A. & Zagorchev, I., 2004. Transect VII: East European Craton – Scythian Platform – Dobrogea – Balkanides – Rhodope Massif – Hellenides – East Mediterranean – Cyrenaica. in *The TRANSMED Atlas. The Mediterranean Region from Crust to Mantle,* eds Cavazza, W., Roure, F., Spakman, W., Stampfli, G.M. & Ziegler, P.A., Geological and Geophysical Framework, Springer (CDROM content).

Patrut, I., Paraschiv, C. & Danet, T., 1983. The geological constitution of the Danube Delta, *An. Inst. Geol. Geof.,* **LIX,** 55–62.

Pavlenkova, N.I., 1996. Crust and Upper Mantle Structure in Northern Eurasia from Seismic Data, in *Advances in Geophysics,* Vol. 37, pp. 3–133, eds Dmovska, R. & Altzman, B.S., Academic Press Inc.

Percival, J.A., Cook, F.A. & Clowes, R.M., 2012. *Tectonic Styles in Canada: The Lithoprobe Perspective,* Geological Survey of Canada, Special Paper 49, 498 pp.

Plakhotny, L.G., Apostolova, M.Ja., Bondarenko, V.G. & Gordievich, V.A., 1971. Cretaceous volcanic of the Crimean Plain, *Bull. Moscow Soc. Naturalists,* **46**(4), 102–112 (in Russian).

Robinson, A.G., Rudat, J.H., Banks, C.J. & Wiles, R.L.F., 1996. Petroleum geology of the Black Sea, *Mar. Petrol. Geol.,* **13,** 195–223.

Rolland, Y., Sosson, M., Adamia, S. & Sadradze, N., 2011. Prolonged 'Variscan to Alpine' history of Active Eurasian margin (Georgia, Armenia) revealed by 40Ar/39Ar dating, *Gondwana Reserch,* **20**(4), 798–815.

Saintot, A., Stephenson, R.A., Stovba, S., Brunet, M.F., Yegorova, T. & Starostenko, V., 2006. The evolution of the southern margin of Eastern Europe (Eastern European and Scythian platforms) from the latest Precambrian-Early Palaeozoic to the Early Cretaceous, in *European Lithosphere Dynamics, Memoirs,* Vol. 32, pp. 481–505, eds Gee, D.G. & Stephenson, R.A., Geological Society.

Sandrin, A. & Thybo, H., 2008. Seismic constraints on a large mafic intrusion with implications for the subsidence history of the Danish Basin, *J. Geophys. Res.: Solid Earth,* **113,** B09402, doi:10.1029/2007JB005067.

Scheck, M. & Bayer, U., 1999. Evolution of the Northeast German Basin—inferences of a 3D structural model and subsidence analysis, *Tectonophysics,* **373,** 55–73.

Seghedi, A., 2001. The North Dobrogea orogenic belt (Romania): a review, in *Peri-Tethys Memoir 6: PeriTethyan Rift /Wrench Basins and Passive Margins,* Vol. 186, pp. 237–257, eds Ziegler, P.A., Cavazza, W., Robertson, A.F.H. & Crasquin-Soleau, S., Memoires du Museum national d'Histoirenaturelle.

Seghedi, A., 2012. Palaeozoic formations from Dobrogea and Pre-Dobrogea—an overview, *Turkish J. Earth Sci.,* **21,** 669–721.

Sheremet, Ye., Sosson, M., Gintov, O., Müller, C., Yegorova, T. & Murovskaya, A., 2014. Key problems of stratigraphy of Crimean Mountains. New micropaleontological data on flysh rocks, *Geophys. J.,* **2,** 35–56 (in Russian).

Shillington, D.J., Scott, C.L., Minshull, T.A., Edwards, R.A., Brown, P.J. & White, N., 2009. Abrupt transition from magma-starved to magma-rich rifting in the eastern Black Sea, *Geology,* **37**(1), 7–10.

Sidorenko, A.V. (ed.), 1969. *Geology of the USSR. Crimea. Geological description,* Gosgeolizdat, 575 pp. (in Russian).

Slyusar', B.S., 1984. Structures of the horizontal compression in the northern Fore-Dobrudja, *Geotektonika,* **4,** 90–105 (in Russian).

Sokoutis, D., Burg, J.P., Bonini, M., Corti, G. & Cloetingh, S., 2005. Lithospheric-scale structures from the perspective of analogue continental collision, *Tectonophysics,* **406,** 1–15.

Sollogub, V.B., 1986. *Lithosphere of the Ukraine,* Naukova Dumka, 184 pp. (in Russian).

Sollogub, V.B. *et al.*, 1985. The structure of the lithosphere along geotraverse V on the basis of complex geological and geophysical data, *Geophys. J.,* **4,** 3–18 (in Russian).

Sollogub, V.B., 1988a. Lithosphere structure along the geotraverse V, in *Lithosphere of Central and East Europe. Geotraverse I, II, V,* pp. 112–160, ed. Cherunov, A.V., Naukova Dumka (in Russian).

Sollogub, V.B., 1988b. Lithosphere structure along the geotraverse VI, in *Lithosphere of Central and East Europe. Geotraverse IV, VI, VIII,* pp. 67–121, ed. Chekunov, A.V., Naukova Dumka (in Russian).

Sollogub, V.B. *et al.*, 1987. *Geology of the Shelf of the USSR, Tectonics,* Naukova Dumka, 152 pp. (in Russian).

Środa, P. *et al.*, 2006. Crustal and upper mantle structure of the Western Carpathians from CELEBRATION 2000 profiles CEL01 and CEL04: seismic models and geological implications, *Geophys. J. Int.,* **167,** 737–760.

Starostenko, V. *et al.*, 2004. Topography of the crust-mantle boundary beneath the Black Sea Basin, *Tectonophysics,* **381,** 211–233.

Starostenko, V. *et al.*, 2013. Mesozoic(?) lithosphere-scale buckling of the East European Craton in southern Ukraine: DOBRE-4 deep seismic profile, *Geophys. J. Int.,* **195,** 740–766.

Starostenko, V. *et al.*, 2014. Thermal structure of the crust in the Black Sea: comparative analysis of magnetic and heat flow data, *Mar. Geophys. Res.,* **35,** 345–359.

Starostenko *et al.*, 2015. DOBRE-2 WARR profile: the Earth's crust across Crimea between the pre-Azov Massif and the northeastern Black Sea Basin, in Geological Society, Special Publications, in press.

Stephenson, R. & Cloetingh, S., 1991. Some examples and mechanical aspects of continental lithospheric folding, *Tectonophysics,* **188,** 27–37.

Stephenson, R., Mart, Y., Okay, A.I., Robertson, A., Saintot, A., Stovba, S. & Khriachtchevskaia, O., 2004. TRANSMED transect VIII: eastern European Craton-Crimea-Black Sea-Anatolia-Cyprus-Levant-Sea-Sinai-Red Sea, in *The TRANSMED Atlas – The Mediterranean Region from Crust to Mantle: Geological and Geophysical Framework of the Mediterranean and the Surrounding Areas,* pp. 141, eds Cavazza, W., Roure, F.M., Spakman, W., Stampfli, G.M. & Ziegler, P.A., Springer.

Thybo, H., 2000. Crustal structure and tectonic evolution of the Tornquist Fan region as revealed by geophysical methods, *Bull. Geol. Soc. Denmark,* **46,** 145–160.

Thybo, H. & Artemieva, I.M., 2013. Moho and magmatic underplating in continental lithosphere, *Tectonophysics,* **609,** 605–619.

Thybo, H. & Nielsen, C.A., 2009. Magma-compensated crustal thinning in continental rift zones, *Nature,* **457,** 873–876.

Thybo, H. & Schonharting, G., 1991. Geophysical evidence for Early Permian igneous activity in a transtensional environment, Denmark, *Tectonophysics,* **189,** 193–208.

Thybo, H., Maguire, P.K.H., Birt, C. & Perchuc, E., 2000. Seismic reflectivity and magmatic underplating beneath the Kenya Rift, *Geophys. Res. Lett.,* **27,** 2745–2748.

Thybo, H. *et al.*, 2003. Upper lithospheric seismic structure across the Pripyat Trough and the Ukrainian Shield along the EUROBRIDGE'97 profile, *Tectonophysics,* **371,** 41–79.

Tugolesov, D.A., Gorshkov, A.S., Meisner, L.B. & Khakhalev, E.M., 1985. *Tectonics of Mesozoic-Cenozoic Successions of the Black Sea Basin,* Nedra, 215 pp. (in Russian).

Wessel, P. & Smith, W.H.F., 1995. New version of the Generic Mapping Tools released, *EOS, Trans. Am. geophys. Un.,* **76,** 329.

Yegorova, T. & Gobarenko, V., 2010. Structure of the Earth's crust and upper mantle of West- and East-Black Sea Basins revealed from geophysical data and its tectonic implications, in *Sedimentary Basin Tectonics from the Black Sea and Caucasus to the Arabian Platform,* Vol. 340, pp. 23–42, eds Sosson, M., Kaymakci, N., Stephenson, R., Bergerat, F. & Starostenko, V., Geological Society, Special Publications.

Yegorova, T., Gobarenko, V. & Yanovskaya, T., 2013. Lithosphere structure of the Black Sea from 3D gravity analysis and seismic tomography, *Geophys. J. Int.,* **193,** 287–303.

Yegorova, T.P., Starostenko, V.I., Kozlenko, V.G. & Yliniemi, J., 2004. Lithosphere structure of the Ukrainian Shield and Pripyat Trough in the region of EUROBRIDGE-97 (Ukraine and Belarus) from gravity modeling, *Tectonophysics,* **381,** 29–59.

Yegorova, T.P., Baranova, E.P. & Omelchenko, V.D., 2010. The crustal structure of the Black Sea from reinterpretation of Deep Seismic Sounding data acquired in the 1960s, in *Sedimentary Basin Tectonics from the Black Sea and Caucasus to the Arabian Platform,* Vol. 340, pp. 43–56, eds Sosson, M., Kaymakci, N., Stephenson, R., Bergerat, F. & Starostenko, V., Geological Society, Special Publications.

Yudin, V.V., 2008. *Geodynamics of the Black Sea-Caspian Region,* UkrDGRI, 117 pp. (in Russian).

Zakariadze, G., Dilek, Y., Adamia, S., Oberhänsli, R., Karpenko, S., Bazylev, B. & Solov'eva, N., 2007. Geochemistry and geochronology of the Neoproterozoic Pan-African Transcaucasian Massif

(Republic of Georgia) and implications for island-arc evolution of the late Precambrian Arabian-Nubian Shield, *Gondwana Res.,* **11,** 97–108.

Zelt, C.A., 1994. *Software Package ZPLOT,* Bullard Laboratories, University of Cambridge.

Ziegler, P.A., Cloetingh, S. & van Wees, J-D., 1995. Dynamics of intraplate compressional deformation: the Alpine foreland and other examples, *Tectonophysics,* **252,** 7–59.

Zonenshain, L.P., Kuzmin, M.I. & Natapov, L.M., 1990. Tectonic framework, in *Geology of the USSR: A Plate Tectonics Synthesis,* Geophysics Geodynamics Series, Vol. 21, pp. 242, ed. Page, B.M., American Geophysical Union.